European Journal of Medicinal Chemistry 217 (2021) 113351

Contents lists available at ScienceDirect

European Journal of Medicinal Chemistry

journal homepage: http://www.elsevier.com/locate/ejmech

Comprehensive study on potent and selective carbonic anhydrase inhibitors: Synthesis, bioactivities and molecular modelling studies of 4-(3-(2-arylidenehydrazine-1-carbonyl)-5-(thiophen-2-yl)-1*H*-pyrazole-1-yl) benzenesulfonamides

Cem Yamali [a, b], Hiroshi Sakagami [c], Yoshihiro Uesawa [d], Kota Kurosaki [d], Keitaro Satoh [e], Yoshiko Masuda [f], Satoshi Yokose [g], Abdulilah Ece [h], Silvia Bua [i], Andrea Angeli [i], Claudiu T. Supuran [i], Halise Inci Gul [a, *]

[a] Department of Pharmaceutical Chemistry, Faculty of Pharmacy, Ataturk University, Erzurum, Turkey
[b] Department of Basic Pharmaceutical Sciences, Faculty of Pharmacy, Cukurova University, Adana, Turkey
[c] Research Institute of Odontology (M-RIO), Meikai University, Saitama, Japan
[d] Department of Medical Molecular Informatics, Meiji Pharmaceutical University, Tokyo, Japan
[e] Division of Pharmacology, Meikai University School of Dentistry, Saitama, Japan
[f] Department of Operative Dentistry, Matsumoto Dental University, Nagano, Japan
[g] Division of Endodontics and Operative Dentistry, Meikai University School of Dentistry, Sakado, Saitama, Japan
[h] Department of Pharmaceutical Chemistry, Faculty of Pharmacy, Biruni University, Istanbul, Turkey
[i] Neurofarba Department, Sezione di Scienza Farmaceutiche e Nutraceutiche, Universita Degli Studi di Firenze, Via U. Schiff 6, 50019, Sesto Fiorentino, Florence, Italy

ARTICLE INFO

Article history:
Received 11 January 2021
Received in revised form
21 February 2021
Accepted 27 February 2021
Available online 6 March 2021

Keywords:
Carbonic anhydrase
hCA IX
Anticancer
OSCC
Apoptosis
Pyrazole
Benzenesulfonamide
Hydrazone
Docking

ABSTRACT

In this research, rational design, synthesis, carbonic anhydrases (CAs) inhibitory effects, and cytotoxicities of the 4-(3-(2-arylidenehydrazine-1-carbonyl)-5-(thiophen-2-yl)-1*H*-pyrazole-1-yl)benzenesulfonamides **1**–**20** were reported. Compound **18** (Ki = 7.0 nM) was approximately 127 times more selective cancer-associated hCA IX inhibitor over hCA I, while compound **17** (Ki = 10.6 nM) was 47 times more selective inhibitor of hCA XI over hCA II compared to the acetazolamide. Compounds **11** (CC_{50} = 5.2 μM) and **20** (CC_{50} = 1.6 μM) showed comparative tumor-specificity (TS= > 38.5; >128.2) with doxorubicin (TS > 43.0) towards HSC-2 cancer cell line. Western blot analysis demonstrated that **11** induced slightly apoptosis whereas **20** did not induce detectable apoptosis. A preliminary analysis showed that some correlation of tumor-specificity of **1**–**20** with the chemical descriptors that reflect hydrophobic volume, dipole moment, lowest hydrophilic energy, and topological structure. Molecular docking simulations were applied to the synthesized ligands to elucidate the predicted binding mode and selectivity profiles towards hCA I, hCA II, and hCA IX.

1. Introduction

Despite the valuable progress in the survival of cancer patients, cancer is still one of the deathful and rising public health concerns. In 2018, nearly 10 million patients died due to cancer, and it is also predicted that new cancer cases will be around 29–37 million by 2040 [1]. Many of the chemotherapeutic anticancer drugs used in the clinic also have severe side effects [2]. Therefore, there is an ongoing need to develop novel anticancer agents with fewer side effects that may act by different mechanisms of actions and to find out new cancer biomarkers or pathways that have a crucial role throughout the cancer process.

As an attractive superfamily of enzymes in many organisms, carbonic anhydrases (CAs, EC 4.2.1.1) generally include a tightly bound Zn^{2+} ion that interacts with water and histidine molecules at the active site of the enzyme. The function of Zn^{2+} ion is to bind and activate water molecule to catalyze the reversible hydration reaction of carbon dioxide into bicarbonate and proton ions as in

* Corresponding author.
E-mail address: incigul1967@yahoo.com (H.I. Gul).

https://doi.org/10.1016/j.ejmech.2021.113351
0223-5234/

equation $CO_2 + H_2O \leftrightarrows HCO_3^- + H^+$ by a metal hydroxide nucleophilic mechanism. CAs isoenzymes are significant cellular targets for many pathological processes and pharmacological applications such as anticonvulsants, diuretics, antiglaucoma, anticancer agents, and diagnostic tools for imaging hypoxic tumors [3].

In the members of the superfamily α-CAs in mammals, which differ by features, cellular distribution, expression levels, and response to different classes of inhibitors, especially the hypoxia-induced transmembrane CA IX isoenzyme, along with the transmembrane CA XII isoenzyme, has been approved as promising cancer biomarkers as key pH regulators at the cancer process [4]. The lack of oxygen called hypoxia regulates the expression of several enzymes or transporters by the hypoxia-inducible factor 1 (HIF1) cascade [5,6]. Since hypoxia-inducible CA IX is an effective isoenzyme for the conversion of CO_2 in bicarbonate and proton ions, it also contributes to the acidification of the tumor environment [6]. Because approximately 70% of the hypoxic tumors overexpress CA IX isoenzyme, the cancer cells show unfavorable response to the classical chemotherapies and radiotherapies due to increased resistance or several undesired pathways [7]. Whereas cancer-associated CAs are expressed in a limited amount in normal tissues, they are upregulated or overexpressed in tumor cells such as colon, pancreas, breast, brain, head and neck cancers, squamous/basal cell carcinomas [8,9]. Besides, there are numerous studies on the role of CA IX in oral oncogenesis as a predictor for oral squamous cell carcinomas (OSCC) [10,11]. Hypoxia is also known as one of the important symptoms in OSCC, and novel molecular hallmarks are needed to understand the process of OSCC [12]. Even different results are reported, some studies found out a relationship between the expression level of CA IX in OSCC as a prognostic biomarker [11,13,14]. According to recent studies reported by our research group, several CA IX and/or CA XII inhibitors showed promising *in vitro* cytotoxicities in OSCC cell lines [15–18].

On the other hand, off-target CA I and CA II isoenzymes, which express in red blood cells, cause problematic issues since CA IX and CA XII isoenzymes have approximately 34% similarity with CA II isoenzyme. Therefore, CA I and CA II isoenzymes may reduce the bioavailability of the non-selective CA IX and CA XII inhibitors [19–21]. The properties of the most studied CA I, CA II, and CA IX isoenzymes were given in Table 1 [22]. Based on the findings, the main drawback for developing anticancer drug candidates targeting cancer-associated CAs is known as selective inhibition [21].

The well-known selective anticancer drug candidate is the sulfonamide derivative SLC- 0111 (Fig. 1), an effective inhibitor of CA IX and CA XII, which was forwarded in further clinical studies [23,24]. SLC-0111, which has ureido linker between the zinc-binding group (ZBG) benzenesulfonamide and the tail of the inhibitor, was designed using the well-known tail approach. This linker moiety led to enhance the flexibility of the tail part of the compound to interact with the individual residues of the active site and also tail part of the compound provides isoenzyme specificity over the off-target isoenzymes [8,25]. Hydrazone group as a bioisosteric group of urea is reported as a tailing linker in several benzenesulfonamide derivatives, which is the most effective class of CA inhibitors [19]. The hydrazone linker can also improve the flexibility of the compound to improve the selectivity of the compounds towards hCA IX by leading to favorable interactions with the specific residues of the enzyme [25].

Reported CAs inhibitors having a similar chemical structure to the present study were shown in Fig. 1. In previous studies reported by our group, pyrazoline-benzenesulfonamides including thiophen ring **1** were declared as a selective inhibitor of cancer-related hCA XII isoenzyme with the selectivity values of hCA I/hCA XII = 1250 and hCA II/hCA XII = 224 (Fig. 1) [17]. In another study, some 1,3,5-trisubstituted pyrazole-benzenesulfonamides incorporating hydrazine moiety were also reported as selective hCA IX inhibitors. In that study, the compound **2** having thiophen ring showed moderate selectivity towards hCA IX with the selectivity values of hCA I/hCA IX = 4.6 and hCA II/hCA IX = 0.9 (Fig. 1) [18]. Sharma V et al. [26] reported the inhibition potential of the compound **3**, trifluoromethylhydrazone-carbonyl-1,2,3-triazole containing benzenesulfonamide (Fig. 1) against tumor-associated hCA IX with the value of Ki = 1.4 nM. Allam HA et al. [20] reported hydrazone derivatives incorporating benzenesulfonamide moiety, **4** (Fig. 1), as CAIs, in the range of 3.1–23.7 nM towards hCA IX. Yazıcı-Demir K et al. [27] reported indole-based sulfonamide derivatives **5** (Fig. 1) having hydrazone moiety as selective CAIs with Ki value of 9.2–476.1 nM (hCA IX) and 1.4–219.7 nM (hCA XII). Based on the studies, it can be expressed that using heterocyclic rings and/or hydrazone moiety incorporating benzenesulfonamide can be considered as one of the modifications to increase the isoenzyme selectivity.

Numerous studies and our previous experiences pointed out that heterocyclic ring bearing sulfonamides/benzenesulfonamides are an attractive group of compounds with their significant CAs inhibitory activity profiles and anticancer effects as mentioned above. As a part of our ongoing studies to develop potent and selective enzyme inhibitors targeting the cancer-related hCA IX isoenzyme, herein, we designed and synthesized a class of hydrazone derivatives incorporating pyrazole-benzenesulfonamide (Scheme 1) to evaluate *in vitro* biological effects towards hCA I, hCA II, hCA IX, and OSCC cell lines. Furthermore, mechanism of action studies, molecular docking, and QSAR studies were applied.

2. Results and discussion

2.1. Chemistry

A wide range of bioactivities of hydrazones makes them a popular compound class in drug design and development studies as well as in

Table 1
The properties of the most studied human CAs [22].

	Organ/Tissue Distribution	Subcellular Localization	Catalytic Activity (CO_2 Hydration)	Affinity for Sulfonamides	Target Diseases
CAI	erythrocytes gastrointestinal tract eye	cytosol	low	medium	retinal cerebral edema
CA II	erythrocytes eye gastrointestinal tract bone osteoclasts kidney, lung, testis, brain	cytosol	high	very high	glaucoma edema epilepsy altitude sickness
CA IX	tumors gastrointestinal mucosa	transmembrane	high	high	cancer

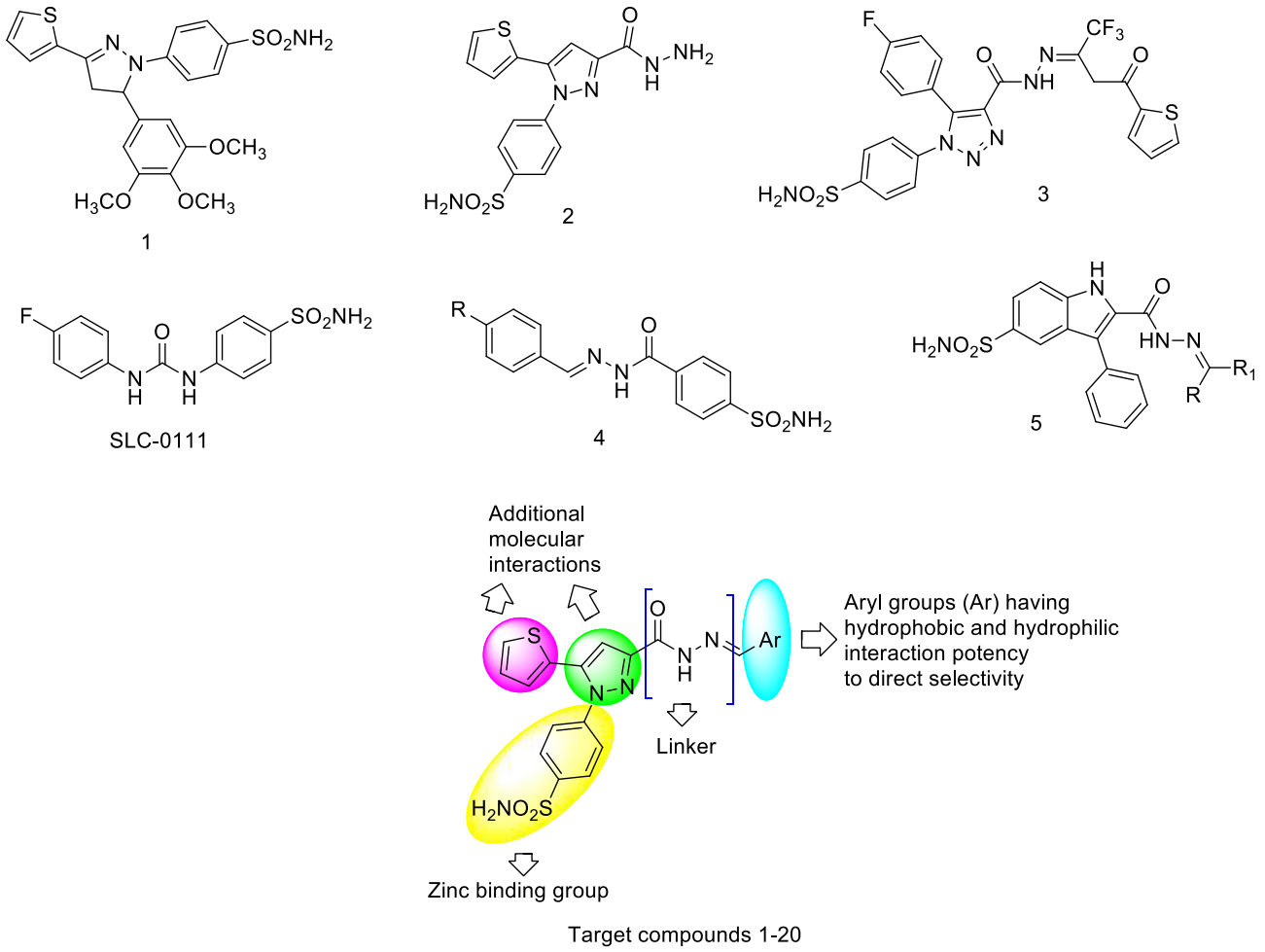

Fig. 1. Chemical structure of the potent CAs inhibitors and target compounds **1**–**20**.

synthetic chemistry [28,29]. The synthesis pathway of the hydrazone derivatives of pyrazole-benzenesulfonamide is presented in Scheme 1. Synthesis of the starting compound 4-(3-(hydrazinecarbonyl)-5-(thiophene-2-yl)-1*H*-pyrazole-1-yl)benzenesulfonamide (**I3**) and its structural analysis were reported in our previous studies [18,30]. In this study, twenty compounds were synthesized and their structures were confirmed by ^{1}H NMR, ^{13}C NMR, and HRMS. Spectras can be found in the supplementary file. According to NMRs data, a proton signal of the functional −N═CH- group was seen in the range of δ 8.83–8.35 ppm while another proton belongs to −CONH− moiety was observed at δ 12.15–11.49 ppm as a singlet. $-NH_2$ protons belonging sulfonamide group also was generally seen as a singlet in the range of δ 7.56–7.52 ppm. A signal that belongs to the proton at the fourth position of the pyrazole ring was seen in the field of δ 7.29–7.18 ppm in singlet appearance, except the compounds 4-methyl and 4-fluoro derivatives. Methoxylated and methylated compounds had also signals for aliphatic protons and carbons in the expected areas of the spectra. As a general fact, 4-fluorinated compound **4** gave additional peaks due to strong ^{19}F–^{13}C spin-spin coupling. Therefore, coupling constants $^{1}J_{CF}$ = 247.9 Hz, $^{2}J_{CF}$ = 22.1 Hz, and $^{3}J_{CF}$ = 9.2 Hz were recorded for the 4-fluorinated compound **4**. HRMS results also confirmed the chemical structure of the compounds by the calculated and measured *m*/*z* values of the compounds.

2.2. Carbonic anhydrase inhibition

In this study, *in vitro* enzyme inhibitory effects of the compounds were examined towards cytosolic (human) hCA I and hCA II, and tumor-associated transmembrane hCA IX isoenzymes by a stopped-flow, CO_2 hydrase assay according to previous studies [15–18,31–34]. Inhibition constants (Ki) and selectivity ratios calculated are shown in Table 2. The structure-activity relationship (SAR) analysis was deduced from Table 2. The cytosolic hCA I and hCA II were inhibited by most of the compounds in the high nanomolar range with the inhibition constant (Ki) values ranging from 652 to >10000 nM (hCAI) and 8.9->10000 nM (hCA II) while the reference drug AZA's Ki values were 250 and 12.1 nM, respectively. Compounds generally showed weak activity towards hCA I and hCA II, except compound **19** (Ki = 8.9 nM, hCA II) compared to AZA. Since compound **19** having furan ring was found 7-times more potent than its phenyl analog **1 towards hCA II**, it can be stated here bioisosteric replacement remarkably increased inhibitory potency against hCA II. On the other hand, the substitution of halogens such as fluorine and chlorine generally led to increased activity towards hCA II, except bromine. Electron-releasing methoxy groups dramatically decreased inhibitory potency. Dimethoxy and trimethoxy bearing compounds reduced activity in the range of 13–161 times compared to phenyl analog **1**. The data showed that poly-

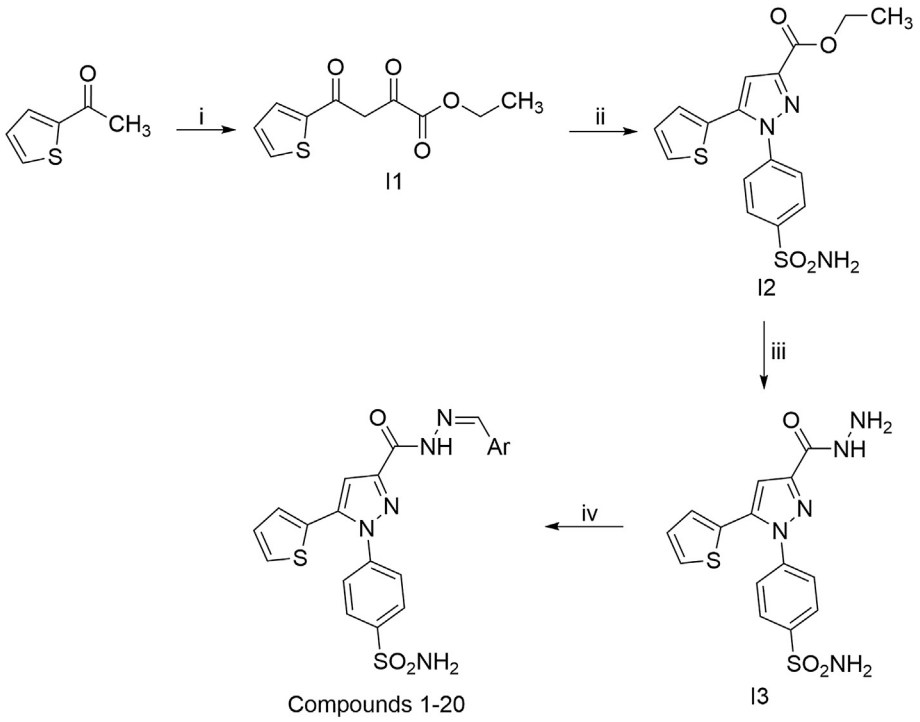

Scheme 1. Synthetic pathway of the target sulfonamides **1**–**20**.
Conditions and reagents: (**i**) NaOEt, diethyloxalate, EtOH, rt. (**ii**) 4-hydrazinobenzensulfonamide hydrochloride, EtOH, reflux. (**iii**) Hydrazine hydrate (99%), MeOH, reflux, (**iv**) Aldehyde derivative, EtOH, gl.HAc, reflux. Ar: Phenyl (**1**), 4-methylphenyl (**2**), 4-methoxyphenyl (**3**), 4-fluorophenyl (**4**), 4-chlorophenyl (**5**), 4-bromophenyl (**6**), 4-nitrophenyl (**7**), 4-trifluoromethylphenyl (**8**), 2,3-dimetoxyphenyl (**9**), 2,4-dimetoxyphenyl (**10**), 2,5-dimetoxyphenyl (**11**), 2,3,4-trimetoxyphenyl (**12**), 3,4,5-trimetoxyphenyl (**13**), 4-dimethylaminophenyl (**14**), 4-hydroxy-3-methoxyphenyl (**15**), 3-hydroxy-4-methoxyphenyl (**16**), 4-hydroxyphenyl (**17**), thiophene-2-yl (**18**), furan-2-yl (**19**), pyridine-4-yl (**20**).

Table 2
hCA I, hCA II, and hCA IX inhibition effects of the compounds **1**–**20**.

Comp.	Ar	Ki (nM)			Selectivity ratio	
		hCA I	hCA II	hCA IX	hCA I/hCA IX	hCA II/hCA IX
1	Phenyl	7188.8	61.9	20	359.4	3.1
2	4-Methylphenyl	8662.2	870.3	588.6	14.7	1.5
3	4-Methoxyphenyl	10000	5660.7	1534.3	6.5	3.7
4	4-Fluorophenyl	5541.7	41.5	15.8	350.7	2.6
5	4-Chlorophenyl	7178.9	40.8	6.7	1071.5	6.1
6	4-Bromophenyl	7034.3	8710.5	1467.1	4.8	5.9
7	4-Nitrophenyl	6612.1	44.3	14	472.3	3.2
8	4-Trifluoromethylphenyl	5517.6	42.3	17.3	318.9	2.4
9	2,3-Dimetoxyphenyl	6456.7	798.6	1787.9	3.6	0.4
10	2,4-Dimetoxyphenyl	>10000	6504.9	1544.9	>6.5	4.2
11	2,5-Dimetoxyphenyl	>10000	4446.8	256.4	>39.0	17.3
12	2,3,4-Trimetoxyphenyl	>10000	>10000	1486.5	>6.7	>6.7
13	3,4,5-Trimetoxyphenyl	>10000	>10000	1778.8	>5.6	>5.6
14	4-Dimethylaminophenyl	7702.9	25.5	13.4	574.8	1.9
15	4-Hydroxy-3-methoxyphenyl	>10000	>10000	1993.7	>5.0	>5.0
16	3-Hydroxy-4-methoxyphenyl	8175.8	53	8.1	1009.4	6.5
17	4-Hydroxyphenyl	8470.5	246.6	10.6	799.1	23.3
18	Thiophene-2-yl	8623.8	58.7	7.0	1232.0	8.4
19	Furan-2-yl	652	8.9	16.8	38.8	0.5
20	Pyridine-4-yl	9650.2	8151.4	789.3	12.2	10.3
	Acetazolamide, AZA	250	12.1	25.8	9.7	0.5

methoxylation of the compounds was not a favorable modification to obtain hCA II inhibitor. As a result, compound **19** (Ki = 8.9 nM) that is the most potent hCA II inhibitor can be considered for glaucoma and epilepsy studies since hCA II has a role in these diseases.

The transmembrane cancer-associated hCA IX isoenzyme was considerably inhibited by the compounds with Ki values in the range of 6.7–1787.9 nM. The following compounds were found as the most effective hCA IX inhibitors compared to AZA (Ki = 25.8 nM): **1**, **4**, **5**, **7**, **8**, **14**, **16**, **17**, **18**, and **19**.

The drawback of finding novel CAIs is mainly the lack of selectivity for a specific CA isoenzyme. Therefore, the selectivity ratios

calculated are given in Table 2. The results showed that some of the compounds had high selectivity in the inhibition of hCA IX over hCA I and hCA II. The following compounds can be considered as the most selective hCA IX inhibitors over hCA I isoenzyme (assessed as the ratio of hCA I/hCA IX): **1** (359.4), **4** (350.7), **5** (1071.5), **7** (472.3), **8** (318.9), **14** (574.8), **16** (1009.4), **17** (799.1), **18** (1232). Among the compounds, **5** having 4-chlorophenyl and **18** having thiophen ring were approximately 110 and 127 times more selective than AZA (hCA I/hCA IX = 9.7). On the other hand, all of the compounds selectively inhibited hCA IX over hCA II, except compounds **9** and **19**. The most selective compounds (assessed by the ratio of hCA II/hCA IX) were **11** (17.3), **17** (23.3), and **20** (10.3). Compound **17** bearing 4-hydroxyphenyl showed 47 times more selective inhibition of hCA IX over hCA II compared to AZA.

According to the SAR analysis, substitution of electron-withdrawing groups such as fluorine, chlorine or nitro and bio-isosteric ring replacements such as thiophen or furan usually increased the enzyme inhibitory potencies of the compounds, while mono or poly methoxylation of the compounds generally decreased activity compared to phenyl derivative towards hCA IX. Substitution of chlorine atom instead of fluorine or bromine led to increasing inhibition potency against hCA IX. The differences may be a result of the atom radius that prevents it from approaching the enzyme. On the other hand, when compounds **3** having methoxy and **17** having hydroxy were compared, the data showed that the hydroxy group increased activity around 145 times towards hCA IX. When vanillin (**15**) and its structural isomer isovanillin (**16**) derivatives were compared, the results also indicated that the hydroxy group at the third position of the phenyl ring increased activity 246 times towards hCA IX. Furthermore, compound **15** having 4-hydroxy-3-methoxyphenyl showed 188 times less activity than **17** having 4-hydroxyphenyl. This data also indicated that the methoxy group at the third position of phenyl ring was not favorable. It can be concluded that the methoxy group made additional hydrogen bond interactions with the hydroxy group, and also the hydroxy group was hindered from interacting with the critical protein residues of the target enzyme. Moreover, thiophen, and furan rings considerably increased inhibitory potency towards hCA XI while pyridine decreased potency compared to phenyl analog **1**.

According to the previous study [18], starting compound 4-(3-(hydrazinecarbonyl)-5-(thiophene-2-yl)-1*H*-pyrazole-1-yl)benzenesulfonamide showed moderate selectivity towards hCA IX with the selectivity values of hCA I/hCA IX = 4.6 and hCA II/hCA IX = 0.9. Converting hydrazine into the hydrazone led to enhanced selectivity for the most of the compounds studied towards hCA IX. Thus, the hydrazone linker was found a useful modification to obtain more powerful and selective hCA IX inhibitors.

When hCA IX inhibitory effects of the drug and/or drug candidates in phase trials as Pazopanib (Ki = 9.1 nM, hCA IX) [35], indisulam (Ki = 24 nM, hCA IX) [35] and SLC-0111 (Ki = 45 nM, hCA IX) [24] were compared with our significant results, compounds **5** (6.7 nM), **18** (7.0 nM), **16** (8.1 nM) and **17** (10.6 nM) with the lowest Ki values can be taken into account as potent, selective and novel hCA IX inhibitors for further *in vivo* experiments.

2.3. Cytotoxicities towards oral squamous cell carcinomas

In vitro cytotoxicities of the compounds, **1**–**20** towards human oral squamous cell carcinoma (OSCC) cell line (HSC-2) and human mesenchymal normal oral cell (human gingival fibroblast, HGF) were investigated according to our previous studies [15,17,18,30,33,36–40]. The 50% cytotoxic concentration (CC_{50}, expressed as μM) of compounds **1**–**20** is determined from the dose-response curve (Fig. 2) and listed in Table 3.

According to the cytotoxicity assay, compound **20** showed the highest cytotoxicity against HSC-2 cells (CC_{50} = 1.6 μM), followed by **17** (2.0 μM) > **11** (5.2 μM) > **12** (18.0 μM) > **8** (19.5 μM) > **4** (24.3 μM) > **2** (31.4 μM). All of the synthesized compounds showed higher cytotoxicity than references 5-FU (CC_{50} > 1000 μM) and MTX (CC_{50} > 400 μM). All of these compounds except doxorubicin did not reduce the viability of tumor cells completely (Fig. 2).

Tumor selectivity (TS) values were calculated by dividing the CC_{50} for HSC-2 by CC_{50} for HGF (B/A in Table 3). Compound **20** showed the highest TS value (>128.2), followed by doxorubicin (>43.0) > **11** (>38.5) > **12** (>11.1) > **8** (>10.3) > **4** (7.2) > **2** (>6.4) > **16** (>6.0) > **18** (>5.5) ≫ 5-FU, methotrexate (><1) (highlighted in Fig. 2). Therefore, compound **20,** having a pyridine ring, was the most selective one compared to the three of the reference drugs.

Further, potency-selectivity expression (PSE) values were calculated by dividing TS by CC_{50} for HSC-2 and then mulptiplied by 100 [(B/A^2)x100 in Table 3], in an attempt to find out the most favorable anticancer compounds having both potency and selectivity. Doxorubicin showed the highest PSE value (>19229.7), followed by **20** (>8218.3) > **11** (>744.2) > **17** (171.1) > *12* (>61.7) > **8** (>52.8) > **4** (29.6) > **2** (>20.2) > **16** (>18.3) > **18** (>15.0) > > methotrexate (><0.25) > 5-FU (><0.1). The compounds **11** with thiophen ring, [CC_{50} (5.2 μM), TS (>38.5), PSİ (>744.2)] and **20** with pyridine ring, [CC_{50} (1.6 μM), TS (>128.2), PSİ (>8218.3)] made great attraction according to their TS and PSE values.

Western blot analysis was carried out to clarify the mechanism of action of the compounds. The results showed that representative compound **11** induced only minor apoptosis (caspase activation assessed by the production of cleaved poly (ADP-ribose) polymerase (PARP) and cleaved caspase-3). On the other hand, compound **20** did not induce apoptosis (Fig. 4). The data showed that apoptotic cell death was not the main pathway for these compounds, most possibly causing other types of cell death or growth arrest in a certain phase of the cell cycle.

The following SAR analysis was inferred from the Ki, TS, and PSE values of the compounds compared to unsubstituted phenyl derivative **1**. Methoxylation of the compounds generally decreased cytotoxicity, except **11** having 2,5-dimetoxyphenyl and **12** having 2,3,4-trimetoxyphenyl. Compound **11** was one of the promising cytotoxic agents with high cytotoxicity and selectivity. In halogen derivatives, fluorinated compounds **4** and **8** showed approximately 2 and 3 times elevated cytotoxicity, while the compounds having bromine (**6**) and chlorine (**5**) were the weakest compounds towards HSC-2. Compound **16** carrying isovanillin was more cytotoxic and selective agent than its structural isomer vanillin derivative **15** in a similar manner with their effects on hCA IX. Converting the phenyl group into phenol dramatically increased cytotoxicity around 27 times. Further, phenol derivative was also more cytotoxic than vanillin and isovanillin derivatives. The data proved that free phenol function is one of the suitable modifications to increase cytotoxicity as similar as its hCA IX effects. Bioisosteric replacement is generally caused by increasing cytotoxicity. Thiophen and pyridine rings were more favorable than the furan ring compared to phenyl derivative. According to cytotoxicity results, the most active compound was **20** having a pyridine ring. The pyridine ring led to enhancing cytotoxicity 33 times compared to phenyl derivative **1**. Also, its PSE value was 1157 times higher than that of **1**.

Moreover, a preliminary QSAR analysis was made to understand correlations between tumor-specificity of compounds and several chemical descriptors. The graphs showed that there were some correlations with several chemical descriptors for vsurf_D7 (hydrophobic volume) (r^2 = 0.271, p = 0.019), dipoleX (The x component of the dipole moment) (r^2 = 0.241, p = 0.028), vsurf_D8 (hydrophobic volume) (r^2 = 0.221, p = 0.037), vsurf_D6 (hydrophobic volume) (r^2 = 0.217, p = 0.039), vsurf_EWmin1 (lowest hydrophilic energy) (r^2 = 0.212, p = 0.041) and ATSC8c

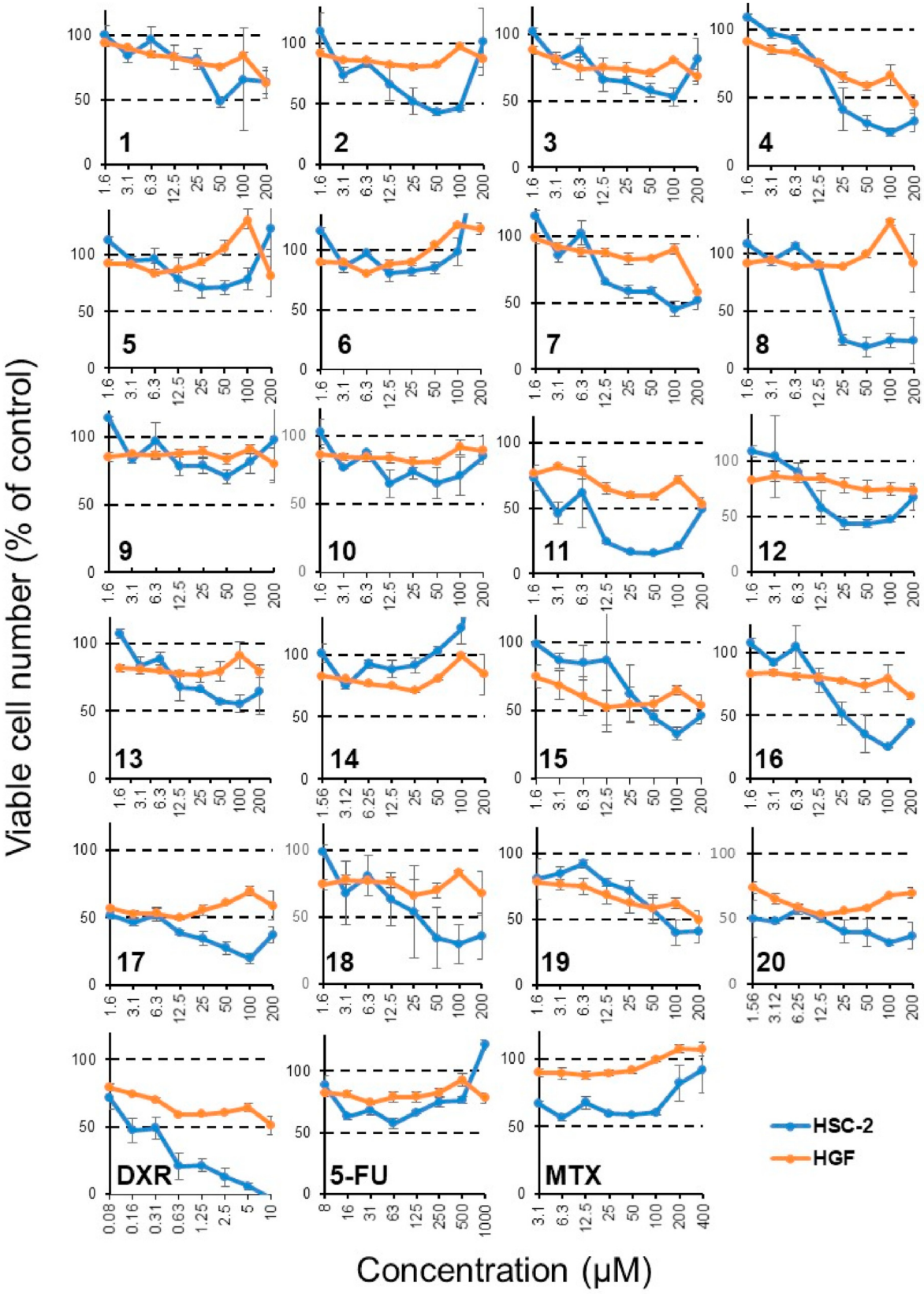

Fig. 2. Dose-response curve for cytotoxicity induced by cytotoxicity of the compounds **1**–**20** towards HSC-2 and HGF cells. Cells were treated for 48 h without (control) with the indicated concentration of samples, and viable cell number was determined by MTT methods. Each value represents the mean ± S.D. of the triplicate assay.

Table 3
Cytotoxicity of the compounds **1**–**20** towards HSC-2 and HGF cells.

Code	Ar	CC_{50} (μM)					
		Malignant		Non-malignant		TS	PSE
		HSC-2	SD	HGF	SD		
		(A)		(B)		(B/A)	$(B/A^2) \times 100$
1	Phenyl	53.0	10.0	>200	0.0	>3.8	>7.1
2	4-Methylphenyl	31.4	15.5	>200	0.0	>6.4	>20.2
3	4-Methoxyphenyl	>158	72.2	>200	0.0	><1.3	><0.8
4	4-Fluorophenyl	24.3	7.0	174.7	32.5	7.2	29.6
5	4-Chlorophenyl	>200	0.0	>200	0.0	><1	><0.5
6	4-Bromophenyl	>200	0.0	>200	0.0	><1	><0.5
7	4-Nitrophenyl	85.1	9.2	>200	0.0	>2.3	>2.8
8	4-Trifluoromethylphenyl	19.5	1.1	>200	0.0	>10.3	>52.8
9	2,3-Dimetoxyphenyl	>200	0.0	>200	0.0	><1	><0.5
10	2,4-Dimetoxyphenyl	>200	0.0	>200	0.0	><1	><0.5
11	2,5-Dimetoxyphenyl	5.2	4.3	>199	2.3	>38.5	>744.2
12	2,3,4-Trimetoxyphenyl	18.0	6.1	>200	0.0	>11.1	>61.7
13	3,4,5-Trimetoxyphenyl	>181	32.9	>200	0.0	><1.1	><0.6
14	4-Dimethylaminophenyl	>200	0.0	>200	0.0	><1	><0.5
15	4-Hydroxy-3-methoxyphenyl	35.1	22.0	23.1	23.4	0.7	1.9
16	3-Hydroxy-4-methoxyphenyl	33.1	15.0	>200	0.0	>6.0	>18.3
17	4-Hydroxyphenyl	2.0	0.4	7.0	4.9	3.5	171.1
18	Thiophene-2-yl	36.5	35.4	>200	0.0	>5.5	>15.0
19	Furan-2-yl	72.1	27.4	145.3	82.9	2.0	2.8
20	Pyridine-4-yl	1.6	0.0	>200	0.0	>128.2	>8218.3
Doxorubicin		0.2	0.2	>9.6	0.7	>43.0	>19229.7
5-Fluorouracil		>1000	0.0	>1000	0.0	><1	><0.1
Methotrexate		>400	0.0	>400	0.0	><1	><0.25

Each value represents the mean from triplicate assays. SD: Standard deviation. TS: Tumor selectivity. PSE: Potency Selectivity Expression.

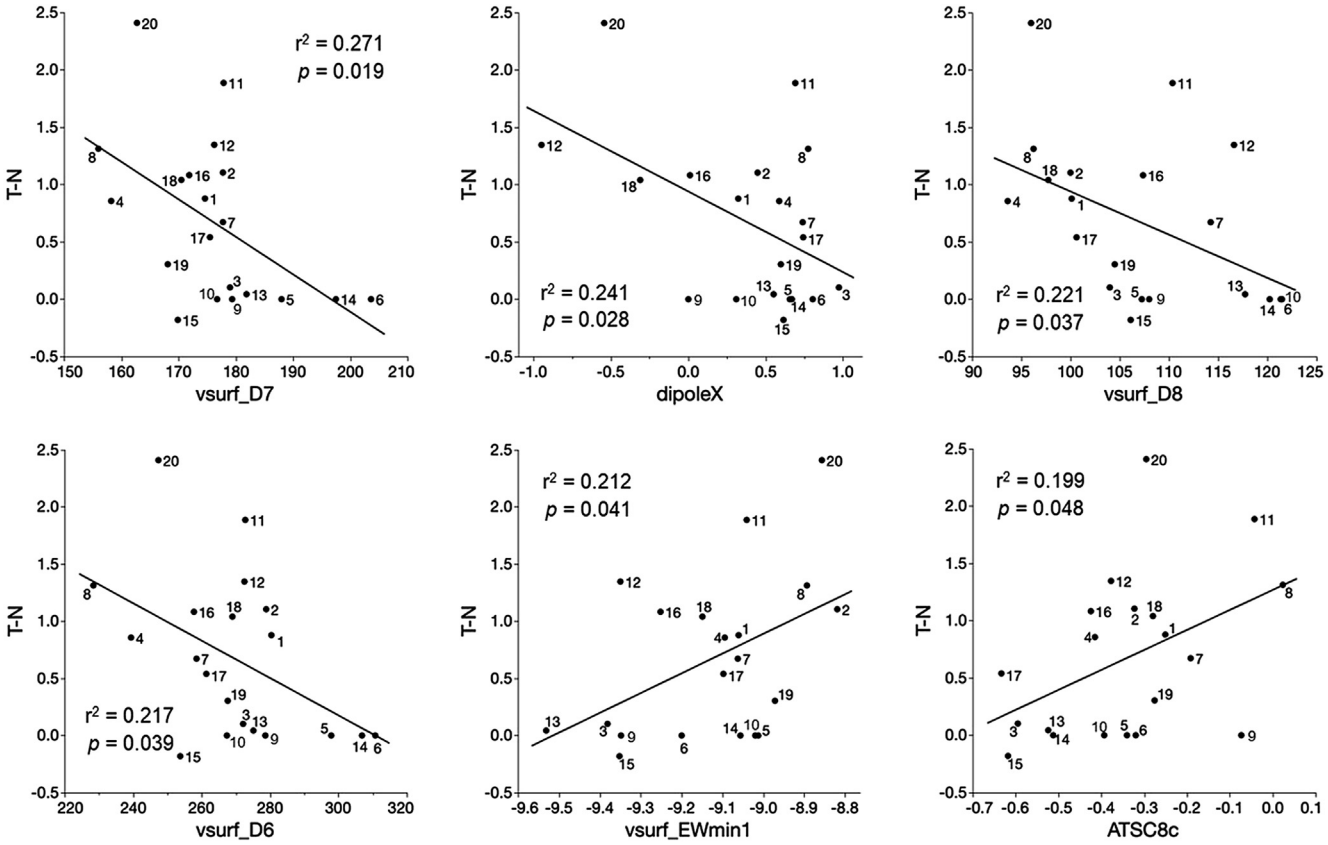

Fig. 3. Top six chemical descriptors that showed correlation with tumor specificity of twenty 4-(3-(2-arylidenehydrazine-1-carbonyl)-5-(thiophen-2-yl)-1*H*-pyrazole-1-yl) benzenesulfonamides.

(autocorrelation of topological structure weighted by gasteiger charge) ($r^2 = 0.199$, $p = 0.048$) (Fig. 3).

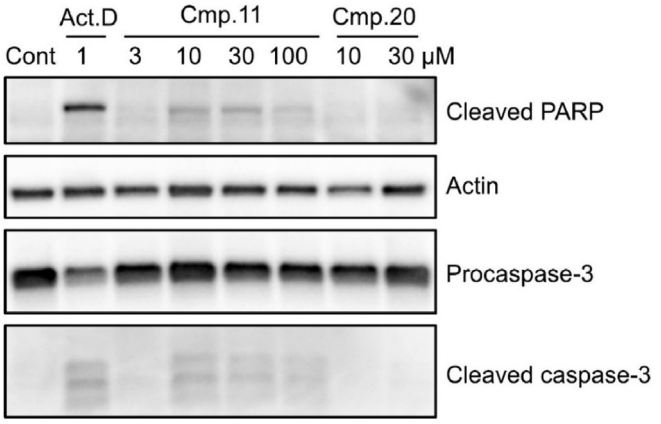

Fig. 4. Western blot analysis for induction of apoptosis by the representative compounds **11** and **20** in HSC-2 cells. The images (long and short exposure) and repeated experiments to check the reproducibility are shown in Supplementary Fig. S1.

It can be expressed here that some of the compounds tested acted as both selective CA IX inhibitors and potent cytotoxic agents. They may show their cytotoxic effects by the inhibition of CA IX isoenzyme as it was mentioned in one of the cancer biomarkers in OSCC, supported by some correlation as shown in Fig. 5. Since this finding is preliminary, further study is needed to confirm the generalization of this finding.

2.4. Molecular docking studies

In order to enlighten inhibition mechanisms of drug candidates with target macromolecules, we often refer to computer-aided drug design techniques that use several approaches involving quantum mechanical calculations or molecular mechanics mainly used in molecular docking simulations [41–43]. In our previous studies, we used several molecular modelling approaches to simulate both biological properties and potential inhibition pathways of novel compounds against a number of therapeutic targets and obtained successful findings [44–48]. Hence, to help us understand and assess the inhibition mechanism and selectivity profiles of the ligands reported here, we have performed molecular docking studies.

Compound **19**, the most active compound against hCA II, adapts a similar binding orientation with AZA by occupying the binding pocket where sulfonamide ring dwells deeply towards gatekeeper residues and Zn^{2+} ion (Fig. 6). It makes favorable hydrogen-bonding interactions with Thr200 and Gln92 and also a π-π interaction is observed between compound **19** and His94 which also plays a critical role in inhibiting hCA II. The furan moiety orients toward the hydrophobic parts of the external part of the cavity. Both thiophene and furan rings seem to have favorable interactions with hydrophobic amino acid residues of hCA II (Pro201-202 and Leu57, Phe70, respectively). We believe that these are key interactions to stabilize **19**-hCA II complex.

On the other hand, the most active compound against hCA IX, compound **5**, was docked in a specific shaped conformation with sulfonamide ring pointing toward the top of the active site (Fig. 7). However, it seems to bind to the Zn^{2+} ion through the carbonyl oxygen to the coordination site of metal ion. The chlorophenyl, thiophene, and also sulfonamide aromatic rings point toward the hydrophobic region of the active site (Pro201, 202, Leu91, 123, 131, 135, 141, Val121, 131). While being in an unusual confirmation, compound **5** keeps known critical interactions with the binding site residues: a hydrogen bond with Thr200 and π-π stacking interaction with His94.

When it comes to the selectivity, compound **17** shows a high selectivity for hCA IX over hCA II. Fig. 8 clearly shows that **17** has different conformations in hCA II and hCA IX binding pockets. The compound **17** is largely stabilized by positioning sulfonamide moiety to the bottom of the binding pocket where it coordinates with Zn metal, makes a hydrogen bond with the gatekeeper residue Thr199 and forms two hydrogen bonds with the neighboring amino acid residue Thr200. Another critical hydrogen bond is observed with Gln92 and also Ala129 which is located at the top of the binding site. Although several interactions are observed between **17** and hCA II, the two hydrogen bonds with Thr200 are absent in **17**-hCA II predicted complex. Instead, a steric clash is observed between this critical amino acid residue (located next to the gatekeeper) and phenol ring of **17**. The sulphonamide ring remains up against the external binding cavity in hCA II. The small hydrophobic residue Val131 at the entrance of the pocket in hCA IX is replaced with a larger residue phenylalanine (Phe131) in hCA II which will make it difficult for large ligands to enter into the active site.

When binding modes of **18**-hCA I is compared with that of hCA IX where a remarkable selectivity is observed, the gatekeeper

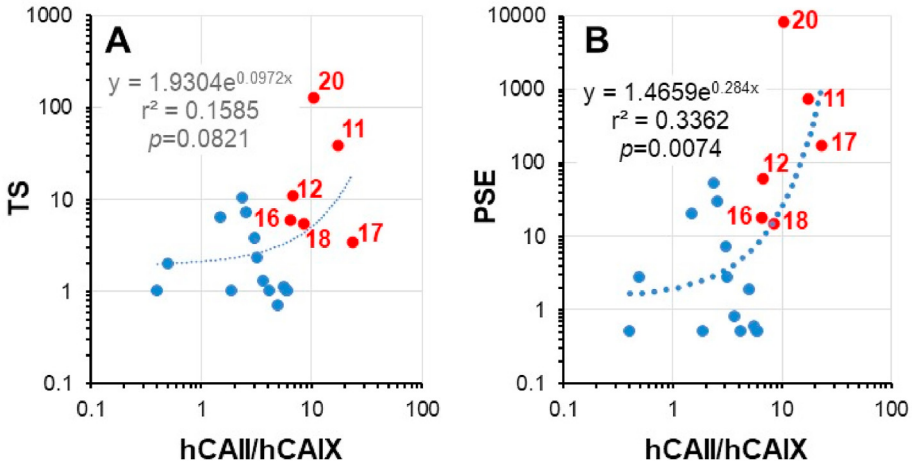

Fig. 5. Correlation of hCAII/hCAIX and TS (A) and PSE (B). The data of hCAII/hCAIX (Table 2) and data of TS or PSE (Table 3) were plotted in logarithmic scale. Red symbols indicates the top six compound with the highest hCAII/hCAIX.

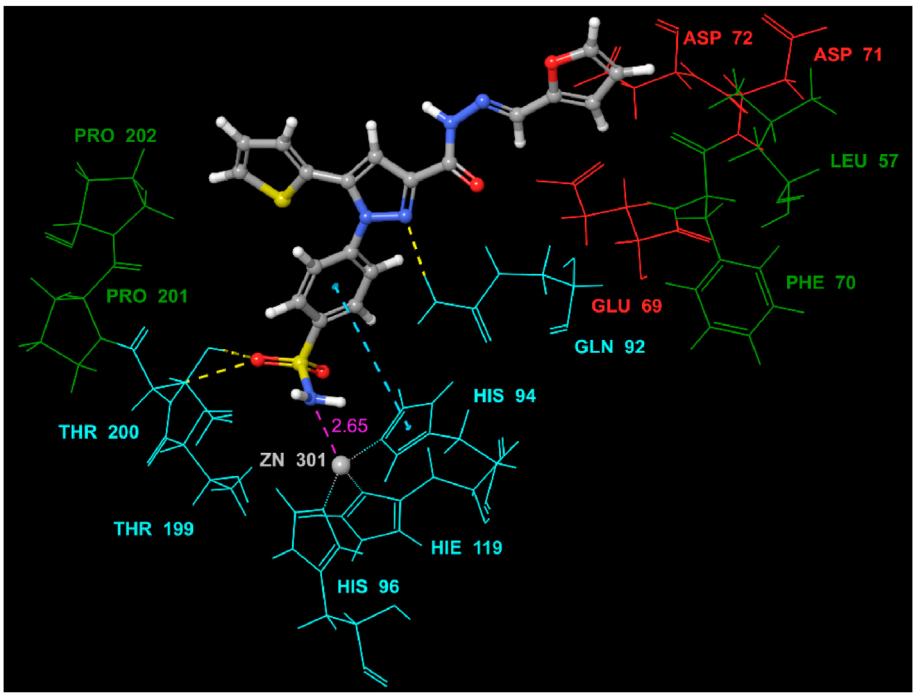

Fig. 6. Calculated 3D binding mode of **19** with hCA II (For the sake of clarity, only discussed residues are shown. Amino acid residues are coloured by properties. Hydrogen bonds: yellow dashed lines; π-π interactions: cyan dashed lines; hydrophobic: green; polar: cyan; negatively charged: red).

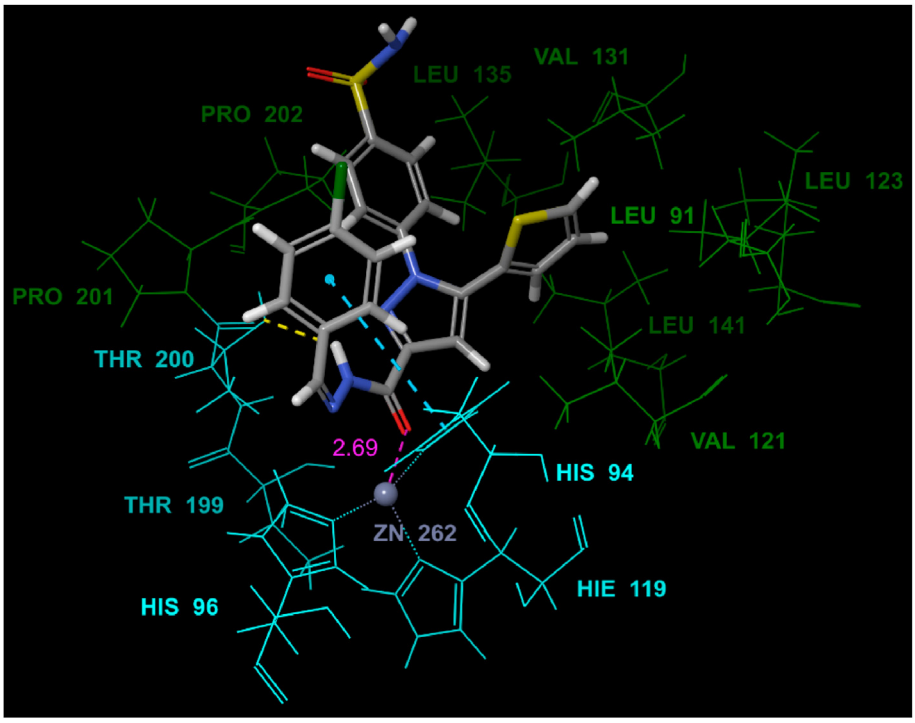

Fig. 7. The docked pose of **5** in the binding pocket of hCA IX (See Fig. 6 for colouring).

residue Thr199 seems to be of significant importance. As shown in Fig. 9, compound **18** interacts with this residue in hCA IX complex by forming two hydrogen bonds while only one hydrogen bond is observed in hCA I binding pocket. It is also noteworthy to mention that the coordination bond distance is significantly shorter between **18** and zinc ion in hCA IX (2.17 vs. 2.60 Å). Those key differences could help to fit **18** in the binding cavity of hCA IX stronger. Although several interactions can be observed in **18**-hCA I complex at a first glimpse, after visual inspection, some steric clashes are observed between **18** and hCA I of which His200 (Thr200 in hCAIX) and His94 are critical residues in enhancing the activities. Hence, unfavorable close contacts with these residues

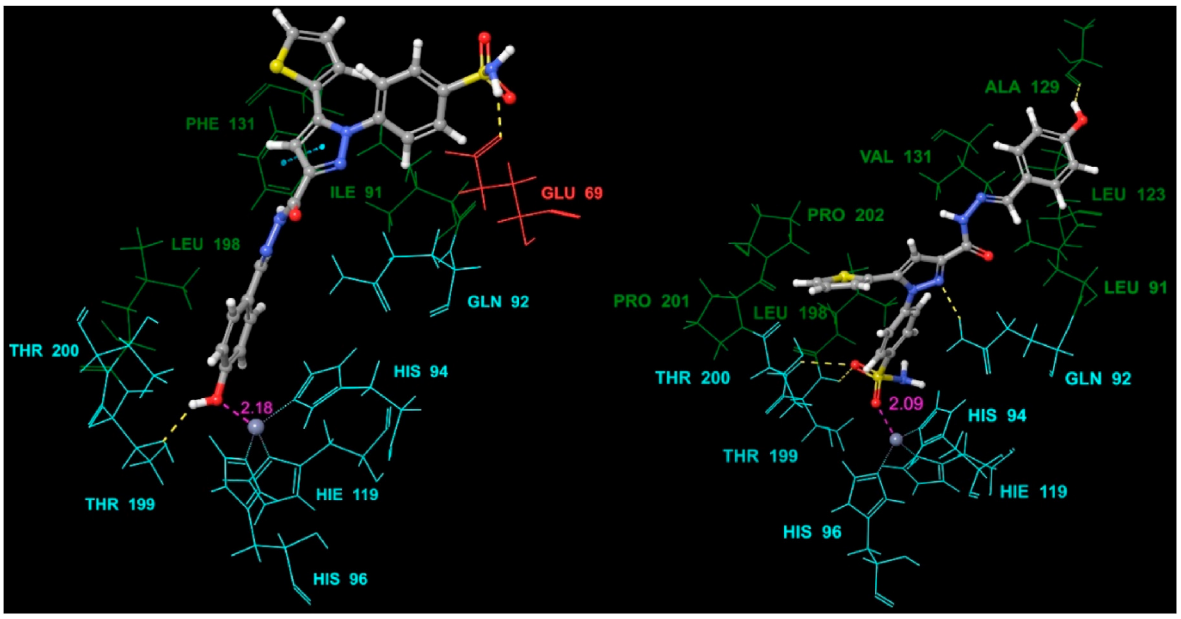

Fig. 8. Comparison of 3D binding mode of **17**-hCA II (left) and **17-**hCA IX (right) complexes (The models are shown in slightly different orientations for clarity. See Fig. 6 for colouring).

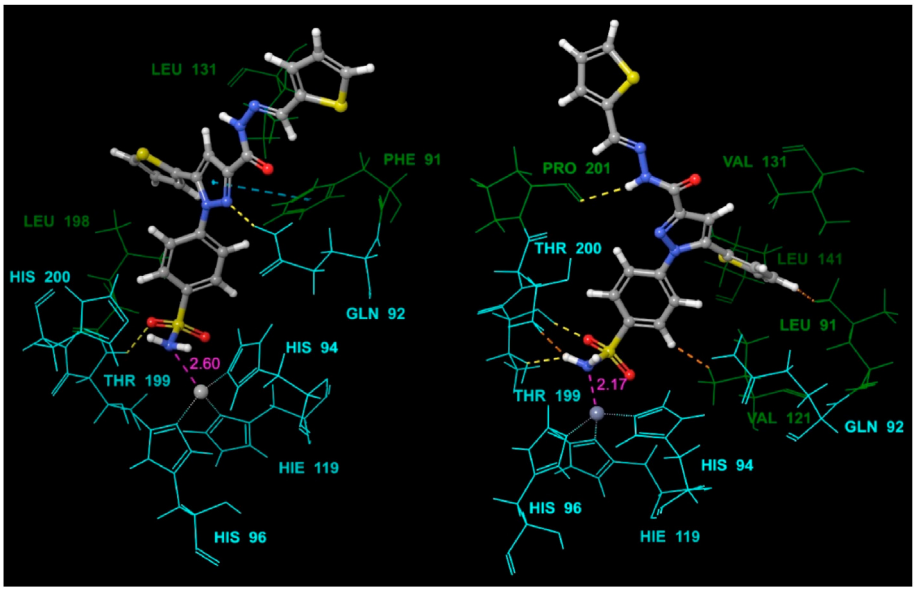

Fig. 9. Comparison of 3D binding mode of **18**-hCA I (left) and **18-**hCA IX (right) complexes (The models are shown in slightly different orientations for clarity. See Fig. 6 for colouring).

appear to not only be detrimental to the activity but it also might block large ligand entry to the active site.

3. Conclusion

In conclusion, compounds **17** (hCA II/hCA IX = 23.3), a 4-hydroxyphenyl derivative, and **18** (hCA I/hCA IX = 1232.0), a thiophen derivative, displayed selective inhibitory potency towards cancer-associated hCA IX over hCA I or hCA II whereas compound **5** (Ki = 6.7 nM), a 4-chlorophenyl derivative, had the lowest Ki values against hCA IX. While compounds **17** (CC_{50} = 2 μM) and **20** (CC_{50} = 1.6 μM) with pyridine moiety showed the highest cytotoxicity against HSC-2 cells, compounds **11** having thiophen with CC_{50} (5.2 μM), TS (>38.5), PSİ (>744.2) values and **20** with CC_{50} (1.6 μM), TS (>128.2), PSİ (>8218.3) values made great attraction according to their TS and PSE values for further investigation. Western blot analysis demonstrated that **11** induced much weaker apoptosis whereas **20** did not induce detectable apoptosis. Enzyme inhibitory potency and cytotoxicities of the compounds were significantly affected by molecular modifications. Besides, molecular modelling analysis helped us to enlighten binding mechanism and selectivity profiles of the ligands which could potentially be considered as lead compounds for further optimization to design more potent and selective hCAs inhibitors.

4. Material and methods

4.1. Chemistry

Nuclear Magnetic Resonance (NMR) spectra (^{1}H NMR and ^{13}C NMR) were recorded with a 400 MHz Varian (Danbury, ABD) spectrometer. DMSO-d_6 (Merck) was used as a solvent. High-Resolution Mass Spectra (HRMS) was recorded taken using a liquid chromatography ion trap-time of the flight tandem mass spectrometer (Shimadzu, Kyoto, Japan) equipped with an electrospray ionization (ESI) source, operating in both positive and negative ionization mode. Shimadzu's LCMS Solution software was used for data analysis. Melting points were determined using an Electrothermal 9100 instrument (IA9100, Bibby Scientific Limited, Staffordshire, UK) and are uncorrected. The process of the reaction was monitored by Thin Layer Chromatography (TLC) using Silicagel HF254 (Merck Art 5715) plate under UV lamb (254 and 365 nm, Spectroline, Model ENF-240C/FE, Spectronics Corporation Westbury, New York U.S.A).

4.1.1. General synthesis method for 4-(3-(2-arylidenhydrazine-1-carbonyl)-5-(aryl)-1H-pyrazole-1-yl) benzenesulfonamides **1**–**20**, Scheme 1

4-(3-(Hydrazinecarbonyl)-5-(thiophene-2-yl)-1*H*-pyrazole-1-yl)benzenesulfonamide (**I3**) was synthesized according to our previous studies [18,30,49]. Briefly, 2,4-dioxo-4-(thiophen-2-yl) butanoate (**I1**) was synthesized by Claisen condensation reaction of the 2-acetyl thiophene with diethyloxalate in the presence of sodium ethoxide. Ethyl 1-(4-sulfamoylphenyl)-5-(thiophen-2-yl)-1*H*-pyrazole-3-carboxylate (**I2**) was obtained by the cyclization of **I1** and 4-hydrazinobenzenesulfonamide hydrochloride by refluxing in ethanol. 4-(3-(Hydrazinecarbonyl)-5-(thiophen-2-yl)-1*H*-pyrazol-1-yl)benzenesulfonamide (**I3**) was synthesized by the refluxing of **I2** and hydrazine hydrate (99%) in ethanol. Details of the synthesis part, ^{1}H NMR, ^{13}C NMR, and HRMS belonging intermediates (**I1**, **I2** and **I3**) were reported in our previous study (18). Compound **I3** was heated in ethyl alcohol: glacial acetic acid (15 ml:0.25 ml) mixture by heating. Then, a suitable aromatic aldehyde derivative was added to the mixture in 1:1 mole ratio. Progress of the reaction was followed by thin-layer chromatography (TLC). Dichloromethane: methanol 4.8:0.2 was used as a mobile phase. The reactions were stopped after a suitable time (varies from 3 h to 24 h). After the reaction solvent is distilled under vacuum up to its half volume, the solid raw product obtained was filtered, and washed with water and then ethanol. The target compounds **1**–**20** were purified by crystallization using methanol/DMF/water (**1**), methanol (**2**), ethanol/DMF (**3** and **4**), methanol/DMF/water (**5**–**20**). Chemical structures of the compounds were enlightened by spectral analysis techniques such as ^{1}H NMR, ^{13}C NMR, and HRMS.

4.1.1.1. 4-(3-(2-(Benzylidene)hydrazine-1-carbonyl)-5-(thiophene-2-yl)-1H-pyrazole-1- yl)benzenesulfonamide, 1. White powder. Yield 23%. Mp = 322–324 °C. ^{1}H NMR (DMSO-d_6, 400 MHz, ppm) δ 11.83 (s, 1H, -CONH), 8.52 (s, 1H, −N=CH-), 7.94 (d, J = 8.8 Hz, 2H, ArH), 7.71 (d, J = 8.8 Hz, 2H, ArH), 7.68–7.65 (m, 3H, ArH), 7.53 (s, 2H, -SO_2NH_2), 7.45–7.42 (m, 3H, ArH), 7.18 (s, 1H, H-4 pyrazole), 7.17 (d, J = 1.0 Hz, 1H, ArH), 7.09 (dd, J = 5.1, 3.7 Hz, 1H, ArH). ^{13}C NMR (DMSO-d_6, 100 MHz, ppm) δ 157.9, 148.9, 147.2, 145.4, 141.9, 139.5, 135.0, 130.8, 129.6, 129.5, 129.4, 128.6, 127.9, 127.8, 127.5, 109.1. HRMS (ESI-MS) *m/z* Calc.: 452.0846 $C_{21}H_{18}N_5O_3S_2$ $[M+H]^+$; Found: 452.0831

4.1.1.2. 4-(3-(2-(4-Methylbenzylidene)hydrazine-1-carbonyl)-5-(thiophene-2-yl)-1H-pyrazole-1- yl)benzenesulfonamide, 2. White powder. Yield 31%. Mp = 257–259 °C. ^{1}H NMR (DMSO-d_6, 400 MHz, ppm) δ 11.76 (s, 1H, -CONH), 8.47 (s, 1H, −N=CH-), 7.94 (d, J = 8.4 Hz, 2H, ArH), 7.70 (d, J = 7.7 Hz, 2H, ArH), 7.66 (d, J = 4.8 Hz, 1H, ArH), 7.57 (d, J = 8.1 Hz, 2H, ArH), 7.53 (s, 2H, -SO_2NH_2), 7.27–7.24 (m, 3H, ArH, H-4 pyrazole), 7.18 (d, J = 3.7 Hz, 1H, ArH), 7.10–7.08 (m, 1H, ArH), 2.33 (s, 3H, −CH_3). ^{13}C NMR (DMSO-d_6, 100 MHz, ppm) δ 157.8, 148.9, 147.3, 145.4, 141.9, 140.6, 139.4, 132.3, 130.1, 129.6, 129.5, 128.6, 127.8, 127.5, 109.1, 21.7. HRMS (ESI-MS) *m/z* Calc.: 466.1002 $C_{22}H_{20}N_5O_3S_2$ $[M+H]^+$; Found: 466.0983

4.1.1.3. 4-(3-(2-(4-Methoxybenzylidene)hydrazine-1-carbonyl)-5-(thiophene-2-yl)-1H-pyrazole-1-yl)benzenesulfonamide, 3. White powder. Yield 68%. Mp = 242–244 °C. ^{1}H NMR (DMSO-d_6, 400 MHz, ppm) δ 11.69 (s, 1H, -CONH), 8.44 (s, 1H, −N=CH-), 7.94 (d, J = 8.4 Hz, 2H, ArH), 7.70 (d, J = 7.7 Hz, 2H, ArH), 7.66 (d, J = 5.1, 1.1 Hz, 1H, ArH), 7.63 (d, J = 8.9 Hz, 2H, ArH), 7.53 (s, 2H, -SO_2NH_2), 7.24 (s, 1H, H-4 pyrazole), 7.17 (dd, J = 3.6, 1.1 Hz, 1H, ArH), 7.09 (dd, J = 5.1, 3.6 Hz, 1H, ArH), 7.00 (d, J = 8.9 Hz, 2H, ArH), 3.79 (s, 3H, −OCH_3). ^{13}C NMR (DMSO-d_6, 100 MHz, ppm) δ 161.6, 157.7, 148.8, 147.4, 145.3, 141.9, 139.4, 129.7, 129.6, 129.4, 128.6, 127.8, 127.6, 127.5, 115.0, 109.1, 56.0. HRMS (ESI-MS) *m/z* Calc.: 482.0951 $C_{22}H_{20}N_5O_4S_2$ $[M+H]^+$; Found: 482.0971

4.1.1.4. 4-(3-(2-(4-Fluorobenzylidene)hydrazine-1-carbonyl)-5-(thiophene-2-yl)-1H-pyrazole-1-yl)benzenesulfonamide, 4. White powder. Yield 77%. Mp = 312–314 °C. ^{1}H NMR (DMSO-d_6, 400 MHz, ppm) δ 11.85 (s, 1H, -CONH), 8.51 (s, 1H, −N=CH-), 7.94 (d, J = 7.7 Hz, 2H, ArH), 7.76–7.70 (m, 4H, ArH), 7.66 (d, J = 5.0 Hz, 1H, ArH), 7.53 (s, 2H, -SO_2NH_2), 7.30–7.25 (m, 3H, ArH, H-4 pyrazole), 7.18 (d, J = 3.7 Hz, 1H, ArH), 7.09 (dd, J = 5.0, 3.7 Hz, 1H, ArH). ^{13}C NMR (DMSO-d_6, 100 MHz, ppm) δ 163.8 ($^1J_{CF}$ = 247.9 Hz), 157.9, 147.8, 147.2, 145.4, 141.8, 139.5, 131.6, 130.0 ($^3J_{CF}$ = 9.2 Hz), 129.6, 129.5, 128.6, 127.8, 127.5, 116.6 ($^2J_{CF}$ = 22.1 Hz), 109.1. HRMS (ESI-MS) *m/z* Calc.: 470.0751 $C_{21}H_{17}N_5O_3FS_2$ $[M+H]^+$; Found: 470.0744

4.1.1.5. 4-(3-(2-(4-Chlorobenzylidene)hydrazine-1-carbonyl)-5-(thiophene-2-yl)-1H-pyrazole-1-yl)benzenesulfonamide, 5. White powder. Yield 48%. Mp = 275–277 °C. ^{1}H NMR (DMSO-d_6, 400 MHz, ppm) δ 11.94 (s, 1H, -CONH), 8.49 (s, 1H, −N=CH-), 7.94 (d, J = 8.4 Hz, 2H, ArH), 7.72–7.69 (m, 4H, ArH), 7.65 (d, J = 5.1 Hz, 1H, ArH), 7.55 (s, 2H, -SO_2NH_2), 7.50 (d, J = 8.4 Hz, 2H, ArH), 7.26 (s, 1H, H-4 pyrazole), 7.18 (d, J = 3.7 Hz, 1H, ArH), 7.08 (dd, J = 5.1, 3.7 Hz, 1H, ArH). ^{13}C NMR (DMSO-d_6, 100 MHz, ppm) δ 157.9, 147.5, 147.1, 145.4, 141.8, 139.5, 135.2, 133.9, 129.7, 129.6, 129.5, 129.4, 128.6, 127.9, 127.5, 109.1, 94.6. HRMS (ESI-MS) *m/z* Calc.: 486.0456 $C_{21}H_{17}N_5O_3S_2Cl$ $[M+H]^+$; Found: 486.0444

4.1.1.6. 4-(3-(2-(4-Bromobenzylidene)hydrazine-1-carbonyl)-5-(thiophene-2-yl)-1H-pyrazole-1-yl)benzenesulfonamide, 6. White powder. Yield 69%. Mp = 278–280 °C. ^{1}H NMR (DMSO-d_6, 400 MHz, ppm) δ 11.91 (s, 1H, -CONH), 8.49 (s, 1H, −N=CH-), 7.94 (d, J = 8.8 Hz, 2H, ArH), 7.70 (d, J = 8.8 Hz, 2H, ArH), 7.67–7.64 (m, 5H, ArH), 7.53 (s, 2H, -SO_2NH_2), 7.26 (s, 1H, H-4 pyrazole), 7.18 (dd, J = 3.7, 1.1 Hz, 1H, ArH), 7.09 (dd, J = 5.1, 3.7 Hz, 1H, ArH). ^{13}C NMR (DMSO-d_6, 100 MHz, ppm) δ 157.9, 147.6, 147.2, 145.4, 141.8, 139.5, 134.3, 132.6, 129.6, 129.5, 128.6, 127.8, 127.5, 124.0, 109.1. HRMS (ESI-MS) *m/z* Calc.: 529.9951 $C_{21}H_{17}N_5O_3S_2Br$ $[M+H]^+$; Found: 529.9944

4.1.1.7. 4-(3-(2-(4-Nitrobenzylidene)hydrazine-1-carbonyl)-5-(thiophene-2-yl)-1H-pyrazole-1-yl) benzenesulfonamide, 7. Yellow powder. Yield 48%. Mp = 307–309 °C. . ^{1}H NMR (DMSO-d_6, 400 MHz, ppm) δ 12.15 (s, 1H, -CONH), 8.62 (s, 1H, −N=CH-), 8.28 (d, J = 9.1 Hz, 2H, ArH), 7.97–7.94 (m, 4H, ArH), 7.72 (d, J = 8.4 Hz, 2H, ArH), 7.66 (dd, J = 5.1, 1.1 Hz, 1H, ArH), 7.54 (s, 2H, -SO_2NH_2), 7.28 (s,

1H, H-4 pyrazole), 7.19 (dd, J = 3.5, 1.1 Hz, 1H, ArH), 7.09 (dd, J = 5.1, 3.5 Hz, 1H, ArH). ^{13}C NMR (DMSO-d_6, 100 MHz, ppm) δ 158.1, 148.6, 146.9, 146.4, 145.5, 141.8, 141.3, 139.6, 129.7, 129.5, 128.7, 128.6, 127.9, 127.5, 124.8, 109.2. HRMS (ESI-MS) *m/z* Calc.: 497.0696 $C_{21}H_{17}N_6O_5S_2$ $[M+H]^+$; Found: 497.0687

4.1.1.8. 4-(3-(2-(4-Trifluoromethylbenzylidene)hydrazine-1-carbonyl)-5-(thiophene-2-yl)-1H-pyrazole-1-yl)benzenesulfonamide, 8. White powder. Yield 63%. Mp = 259–261 °C. ^{1}H NMR (DMSO-d_6, 400 MHz, ppm) δ 12.04 (s, 1H, -CONH), 8.59 (s, 1H, –N=CH-), 7.95 (d, J = 8.8 Hz, 2H, ArH), 7.90 (d, J = 8.1 Hz, 2H, ArH), 7.79 (d, J = 8.4 Hz, 2H, ArH), 7.71 (d, J = 8.4 Hz, 2H, ArH), 7.66 (dd, J = 5.0, 1.2 Hz, 1H, ArH), 7.53 (s, 2H, -SO_2NH_2), 7.28 (s, 1H, H-4 pyrazole), 7.19 (dd, J = 3.6, 1.2 Hz, 1H, ArH), 7.09 (dd, J = 5.0, 3.6 Hz, 1H, ArH). ^{13}C NMR (DMSO-d_6, 100 MHz, ppm) δ 158.1, 147.1, 147.0, 145.4, 141.8, 139.6, 139.0, 130.8, 129.7, 129.6, 129.5, 128.6, 128.4, 127.9, 127.5, 126.5, 109.1. HRMS (ESI-MS) *m/z* Calc.: 520.0719 $C_{22}H_{17}N_5O_3F_3S_2$ $[M+H]^+$; Found: 520.0707

4.1.1.9. 4-(3-(2-(2,3-Dimethoxybenzylidene)hydrazine-1-carbonyl)-5-(thiophene-2-yl)-1H-pyrazole-1-yl)benzenesulfonamide, 9. White powder. Yield 82%. Mp = 245–247 °C. ^{1}H NMR (DMSO-d_6, 400 MHz, ppm) δ 11.94 (s, 1H, -CONH), 8.81 (s, 1H, –N=CH-), 7.95 (d, J = 8.8 Hz, 2H, ArH), 7.71 (d, J = 8.8 Hz, 2H, ArH), 7.65 (dd, J = 5.1, 1.3 Hz, 1H, ArH), 7.56 (s, 2H, -SO_2NH_2), 7.46 (dd, J = 7.1, 2.4 Hz, 1H, ArH), 7.26 (s, 1H, H-4 pyrazole), 7.18 (dd, J = 3.5, 1.3 Hz, 1H, ArH), 7.12–7.08 (m, 3H, ArH), 3.81 (s, 3H, –OCH_3), 3.75 (s, 3H, –OCH_3). ^{13}C NMR (DMSO-d_6, 100 MHz, ppm) δ 157.8, 153.4, 148.8, 147.2, 145.3, 144.6, 141.9, 139.4, 129.7, 129.6, 129.5, 128.6, 127.8, 127.5, 125.1, 117.7, 114.9, 109.1, 61.9, 56.4. HRMS (ESI-MS) *m/z* Calc.: 512.1057 $C_{23}H_{22}N_5O_5S_2$ $[M+H]^+$; Found: 512.1055

4.1.1.10. 4-(3-(2-(2,4-Dimethoxybenzylidene)hydrazine-1-carbonyl)-5-(thiophene-2-yl)-1H-pyrazole-1-yl)benzenesulfonamide, 10. Cream powder. Yield 78%. Mp = 182–184 °C. ^{1}H NMR (DMSO-d_6, 400 MHz, ppm) δ 11.75 (s, 1H, -CONH), 8.75 (s, 1H, –N=CH-), 7.94 (d, J = 8.8 Hz, 2H, ArH), 7.79 (d, J = 9.2 Hz, 1H, ArH), 7.69 (d, J = 8.8 Hz, 2H, ArH), 7.66 (dd, J = 5.0, 1.2 Hz, 1H, ArH), 7.55 (s, 2H, -SO_2NH_2), 7.23 (s, 1H, H-4 pyrazole), 7.16 (dd, J = 3.7, 1.2 Hz, 1H, ArH), 7.09 (dd, J = 5.0, 3.7 Hz, 1H, ArH), 6.61 (d, J = 6.6 Hz, 2H, ArH), 3.83 (s, 3H, –OCH_3), 3.80 (s, 3H, –OCH_3). ^{13}C NMR (DMSO-d_6, 100 MHz, ppm) δ 163.1, 159.9, 157.6, 147.4, 145.2, 144.5, 141.9, 139.2, 129.7, 129.6, 129.4, 128.6, 127.5, 127.4, 115.9, 109.1, 107.0, 98.9, 56.4, 56.1. HRMS (ESI-MS) *m/z* Calc.: 512.1057 $C_{23}H_{22}N_5O_5S_2$ $[M+H]^+$; Found: 512.1042

4.1.1.11. 4-(3-(2-(2,5-Dimethoxybenzylidene)hydrazine-1-carbonyl)-5-(thiophene-2-yl)-1H-pyrazole-1-yl)benzenesulfonamide, 11. Cream powder. Yield 84%. Mp = 199–202 °C. ^{1}H NMR (DMSO-d_6, 400 MHz, ppm) δ 11.92 (s, 1H, -CONH), 8.83 (s, 1H, –N=CH-), 7.94 (d, J = 8.4 Hz, 2H, ArH), 7.70 (d, J = 8.4 Hz, 2H, ArH), 7.66 (dd, J = 5.0, 1.3 Hz, 1H, ArH), 7.55 (s, 2H, -SO_2NH_2), 7.36 (d, J = 3.0 Hz, 1H, ArH), 7.25 (s, 1H, H-4 pyrazole), 7.16 (dd, J = 3.5, 1.3 Hz, 1H, ArH), 7.09 (dd, J = 5.0, 3.5 Hz, 1H, ArH), 7.04–6.99 (m, 2H, ArH), 3.78 (s, 3H, –OCH_3), 3.75 (s, 3H, –OCH_3). ^{13}C NMR (DMSO-d_6, 100 MHz, ppm) δ 157.8, 153.9, 153.1, 147.2, 145.2, 144.3, 141.9, 139.3, 129.7, 129.6, 129.5, 128.6, 127.6, 127.5, 123.7, 118.4, 114.2, 109.8, 109.2, 56.9, 56.2. HRMS (ESI-MS) *m/z* Calc.: 512.1057 $C_{23}H_{22}N_5O_5S_2$ $[M+H]^+$; Found: 512.1055

4.1.1.12. 4-(3-(2-(2,3,4-Trimethoxybenzylidene)hydrazine-1-carbonyl)-5-(thiophene-2-yl)-1H-pyrazole-1-yl)benzenesulfonamide, 12. White powder. Yield 77%. Mp = 248–250 °C. ^{1}H NMR (DMSO-d_6, 400 MHz, ppm) δ 11.83 (s, 1H, -CONH), 8.70 (s, 1H, –N=CH-), 7.94 (d, J = 8.8 Hz, 2H, ArH), 7.71 (d, J = 8.4 Hz, 2H, ArH), 7.65 (dd, J = 5.0, 1.2 Hz, 1H, ArH), 7.61 (d, J = 9.2 Hz, 1H, ArH), 7.55 (s, 2H, -SO_2NH_2), 7.25 (s, 1H, H-4 pyrazole), 7.17 (dd, J = 3.7, 1.2 Hz, 1H, ArH), 7.09 (dd, J = 5.0, 3.7 Hz, 1H, ArH), 6.92 (d, J = 9.2 Hz, 1H, ArH), 3.83 (s, 3H, –OCH_3), 3.81 (s, 3H, –OCH_3), 3.75 (s, 3H, –OCH_3). ^{13}C NMR (DMSO-d_6, 100 MHz, ppm) δ 157.6, 155.8, 153.4, 147.4, 145.3, 144.6, 142.3, 141.9, 139.3, 129.7, 129.6, 129.4, 128.6, 127.8, 127.5, 121.3, 121.2, 109.4, 109.1, 62.6, 61.2, 56.7. HRMS (ESI-MS) *m/z* Calc.: 542.1163 $C_{24}H_{24}N_5O_6S_2$ $[M+H]^+$; Found: 542.1150

4.1.1.13. 4-(3-(2-(3,4,5-Trimethoxybenzylidene)hydrazine-1-carbonyl)-5-(thiophene-2-yl)-1H-pyrazole-1-yl)benzenesulfonamide, 13. White powder. Yield 71%. Mp = 312–314 °C. ^{1}H NMR (DMSO-d_6, 400 MHz, ppm) δ 11.84 (s, 1H, -CONH), 8.42 (s, 1H, –N=CH-), 7.94 (d, J = 8.8 Hz, 2H, ArH), 7.70 (d, J = 8.8 Hz, 2H, ArH), 7.66 (dd, J = 5.0, 1.1 Hz, 1H, ArH), 7.55 (s, 2H, -SO_2NH_2), 7.25 (s, 1H, H-4 pyrazole), 7.18 (dd, J = 3.7, 1.1 Hz, 1H, ArH), 7.09 (dd, J = 5.0, 3.7 Hz, 1H, ArH), 6.96 (s, 2H, ArH), 3.82 (s, 6H, 2x-OCH_3), 3.68 (s, 3H, –OCH_3). ^{13}C NMR (DMSO-d_6, 100 MHz, ppm) δ 157.8, 153.9, 148.9, 147.3, 145.4, 141.8, 139.9, 139.4, 130.5, 129.6, 129.5, 128.6, 127.8, 127.5, 109.1, 104.9, 60.8 (2C), 56.6. HRMS (ESI-MS) *m/z* Calc.: 542.1163 $C_{24}H_{24}N_5O_6S_2$ $[M+H]^+$;Found: 542.1141

4.1.1.14. 4-(3-(2-(4-Dimethylaminobenzylidene)hydrazine-1-carbonyl)-5-(thiophene-2-yl)-1H-pyrazole-1-yl)benzenesulfonamide, 14. Light green powder. Yield 64%. Mp = 252–254 °C. ^{1}H NMR (DMSO-d_6, 400 MHz, ppm) δ 11.49 (s, 1H, -CONH), 8.35 (s, 1H, –N=CH-), 7.94 (d, J = 8.4 Hz, 2H, ArH), 7.69 (d, J = 8.8 Hz, 2H, ArH), 7.65 (dd, J = 5.1, 1.4 Hz, 1H, ArH), 7.53 (s, 2H, -SO_2NH_2), 7.49 (d, J = 8.8 Hz, 2H, ArH), 7.23 (s, 1H, H-4 pyrazole), 7.16 (dd, J = 3.5, 1.4 Hz, 1H, ArH), 7.09 (dd, J = 5.1, 3.5 Hz, 1H, ArH), 6.73 (d, J = 8.8 Hz, 2H, ArH), 2.96 (s, 6H, –$N(CH_3)_2$). ^{13}C NMR (DMSO-d_6, 100 MHz, ppm) δ 157.4, 152.2, 149.7, 147.6, 145.3, 141.9, 139.3, 129.7, 129.5, 129.4, 129.2, 128.6, 127.7, 122.3, 111.5, 109.0. HRMS (ESI-MS) *m/z* Calc.: 495.1268 $C_{23}H_{23}N_6O_3S_2$ $[M+H]^+$; Found: 495.1256

4.1.1.15. 4-(3-(2-(4-Hydroxy-3-methoxybenzylidene)hydrazine-1-carbonyl)-5-(thiophene-2-yl)-1H-pyrazole-1-yl)benzenesulfonamide, 15. White powder. Yield 64%. Mp = 303–305 °C. ^{1}H NMR (DMSO-d_6, 400 MHz, ppm) δ 11.64 (s, 1H, -CONH), 9.27 (s, 1H, –OH), 8.35 (s, 1H, –N=CH-), 7.94 (d, J = 8.8 Hz, 2H, ArH), 7.70 (d, J = 8.8 Hz, 2H, ArH), 7.66 (dd, J = 5.1, 1.1 Hz, 1H, ArH), 7.53 (s, 2H, -SO_2NH_2), 7.24 (d, J = 1.8 Hz, 1H, ArH), 7.23 (s, 1H, H-4 pyrazole), 7.17 (dd, J = 3.7, 1.1 Hz, 1H, ArH), 7.09 (dd, J = 5.1, 3.7 Hz, 1H, ArH), 6.99 (d, J = 1.8 Hz, 1H, ArH), 6.95 (d, J = 8.4 Hz, 1H, ArH), 3.79 (s, 3H, –OCH_3). ^{13}C NMR (DMSO-d_6, 100 MHz, ppm) δ 157.6, 150.5, 149.0, 147.6, 147.4, 145.3, 141.9, 139.4, 129.7, 129.6, 129.4, 128.6, 127.8, 127.7, 127.5, 120.9, 113.0, 112.6, 109.1, 56.3. HRMS (ESI-MS) *m/z* Calc.: 498.0900 $C_{22}H_{20}N_5O_5S_2$ $[M+H]^+$; Found: 498.0888

4.1.1.16. 4-(3-(2-(3-Hydroxy-4-methoxybenzylidene)hydrazine-1-carbonyl)-5-(thiophene-2-yl)-1H-pyrazole-1-yl)benzenesulfonamide, 16. White powder. Yield 59%. Mp = 293–294 °C. ^{1}H NMR (DMSO-d_6, 400 MHz, ppm) δ 11.62 (s, 1H, -CONH), 9.51 (s, 1H, –OH), 8.38 (s, 1H, –N=CH-), 7.94 (d, J = 8.6 Hz, 2H, ArH), 7.69 (d, J = 8.6 Hz, 2H, ArH), 7.55 (dd, J = 5.1, 1.1 Hz, 1H, ArH), 7.52 (s, 2H, -SO_2NH_2), 7.27 (d, J = 1.7 Hz, 1H, ArH), 7.23 (s, 1H, H-4 pyrazole), 7.17 (dd, J = 3.7, 1.1 Hz, 1H, ArH), 7.08 (dd, J = 5.1, 3.7 Hz, 1H, ArH), 7.03 (dd, J = 8.1, 1.7 Hz, 1H, ArH), 6.82 (d, J = 8.1 Hz, 1H, ArH), 3.82 (s, 3H, –OCH_3). ^{13}C NMR (DMSO-d_6, 100 MHz, ppm) δ 157.6, 149.7, 149.5, 148.7, 147.4, 145.3, 141.9, 139.4, 129.7, 129.6, 129.4, 128.6, 127.8, 127.5, 126.4, 122.9, 116.1, 109.6, 56.3. HRMS (ESI-MS) *m/z* Calc.: 498.0900 $C_{22}H_{20}N_5O_5S_2$ $[M+H]^+$; Found: 498.0881

4.1.1.17. 4-(3-(2-(4-Hydroxybenzylidene)hydrazine-1-carbonyl)-5-(thiophene-2-yl)-1H-pyrazole-1- yl)benzenesulfonamide, 17.

White powder. Yield 71%. Mp = >350 °C. ^{1}H NMR (DMSO-d_6, 400 MHz, ppm) δ 11.61 (s, 1H, -CONH), 9.89 (s, 1H, −OH), 8.39 (s, 1H, −N=CH-), 7.94 (d, J = 8.4 Hz, 2H, ArH), 7.70 (d, J = 8.8 Hz, 2H, ArH), 7.64 (dd, J = 5.0, 1.1 Hz, 1H, ArH), 7.53−7.50 (m, 4H, ArH, -SO_2NH_2), 7.23 (s, 1H, H-4 pyrazole), 7.16 (dd, J = 3.6, 1.1 Hz, 1H, ArH), 7.08 (dd, J = 5.0, 3.6 Hz, 1H, ArH), 6.81 (d, J = 8.8 Hz, 2H, ArH). ^{13}C NMR (DMSO-d_6, 100 MHz, ppm) δ 160.1, 157.6, 149.2, 147.5, 145.3, 141.9, 139.3, 129.7, 129.6, 129.4, 128.6, 127.8, 127.5, 125.9, 116.4, 109.0. HRMS (ESI-MS) m/z Calc.: 468.0795 $C_{21}H_{18}N_5O_4S_2$ $[M+H]^+$; Found: 468.0775

4.1.1.18. 4-(3-(2-(Thiophene-2-yl-methylen)hydrazine-1-carbonyl)-5-(thiophene-2-yl)-1H-pyrazole-1-yl)benzenesulfonamide, 18. White powder. Yield 77%. Mp = 314−315 °C. ^{1}H NMR (DMSO-d_6, 400 MHz, ppm) δ 11.86 (s, 1H, -CONH), 8.69 (s, 1H, −N=CH-), 7.94 (d, J = 8.4 Hz, 2H, ArH), 7.70 (d, J = 8.4 Hz, 2H, ArH), 7.66−7.64 (m, 2H, ArH), 7.55 (s, 2H, -SO_2NH_2), 7.39 (dd, J = 3.3, 1.1 Hz, 1H, ArH), 7.23 (s, 1H, H-4 pyrazole), 7.17 (dd, J = 3.3, 1.1 Hz, 1H, ArH), 7.13−7.07 (m, 2H, ArH). ^{13}C NMR (DMSO-d_6, 100 MHz, ppm) δ 157.7, 147.2, 145.4, 143.9, 141.8, 139.8, 139.5, 131.6, 129.7, 129.6, 129.5, 128.6, 127.9, 127.5, 109.1. HRMS (ESI-MS) m/z Calc.: 458.0410 $C_{19}H_{16}N_5O_3S_3$ $[M+H]^+$; Found: 458.0389

4.1.1.19. 4-(3-(2-(Furan-2-yl-methylen)hydrazine-1-carbonyl)-5-(thiophene-2-yl)-1H-pyrazole-1- yl)benzenesulfonamide, 19. Cream powder. Yield 52%. Mp = 291−292 °C. ^{1}H NMR (DMSO-d_6, 400 MHz, ppm) δ 11.86 (s, 1H, -CONH), 8.39 (s, 1H, −N=CH-), 7.94 (dd, J = 8.5, 2.0 Hz, 2H, ArH), 7.83 (s, 1H ArH), 7.71 (dd, J = 8.5, 2.0 Hz, 2H, ArH), 7.65 (dd, J = 4.0, 1.1 Hz, 1H, ArH), 7.55 (s, 2H, -SO_2NH_2), 7.25 (d, J = 2.0 Hz 1H, H-4 pyrazole), 7.18 (dd, J = 3.5, 1.3 Hz, 1H, ArH), 7.08 (dd, J = 4.8, 3.5 Hz, 1H, ArH), 6.88 (dd, J = 3.2 Hz, 1H, ArH), 6.61 (dd, J = 3.2, 1.5 Hz, 1H, ArH). ^{13}C NMR (DMSO-d_6, 100 MHz, ppm) δ 157.8, 150.2, 147.2, 145.9, 145.4, 141.8, 139.5, 138.6, 129.6, 129.5, 128.6, 127.9, 127.5, 114.1, 112.9, 109.0. HRMS (ESI-MS) m/z Calc.: 442.0638 $C_{19}H_{16}N_5O_4S_2$ $[M+H]^+$; Found: 442.0638

4.1.1.20. 4-(3-(2-(Pyridine-4-yl-methylen)hydrazine-1-carbonyl)-5-(thiophene-2-yl)-1H-pyrazole-1- yl)benzenesulfonamide, 20. White powder. Yield 64%. Mp = 310−312 °C. ^{1}H NMR (DMSO-d_6, 400 MHz, ppm) δ 12.15 (s, 1H, CONH), 8.63 (d, J = 4.6 Hz, 2H, ArH), 8.50 (s, 1H, -N=CH-), 7.95 (d, J = 8.4 Hz, 2H, ArH), 7.72 (d, J = 8.4 Hz, 2H, ArH), 7.66 (dd, J = 5.1, 1.1 Hz, 1H, ArH), 7.62 (d, J = 4.6 Hz, 2H, ArH), 7.55 (s, 2H, SO_2NH_2), 7.29 (s, 1H, H-4 pyrazole), 7.19 (dd, J = 3.7 Hz, 1H, ArH), 7.09 (dd, J = 5.1, 3.7 Hz, 1H, ArH). ^{13}C NMR (DMSO-d_6, 100 MHz, ppm) δ 158.1, 150.9, 146.9, 146.5, 145.5, 142.1, 141.8, 139.6, 129.7, 129.5, 128.6, 127.9, 127.5, 121.7, 109.2. HRMS (ESI-MS) m/z Calc.: 453.0798 $C_{20}H_{17}N_6O_3S_2$ $[M+H]^+$; Found: 453.0786

4.2. Carbonic anhydrase inhibition

To assay inhibition effects of the compounds towards hCA I, hCA II, and hCA IX isoenzymes of CAs, an SX.18 MV-R applied photophysics (Oxford, UK) stopped-flow CO_2 hydrase assay was carried out according to previous studies [15−18,31−34].

4.3. Cytotoxic activity and tumor-specificity

Human normal oral mesenchymal cells (human gingival fibroblast, HGF), established from the first premolar tooth extracted from the lower jaw of a 12-year-old girl and human oral squamous cell carcinoma cell line HSC-2 (derived from the tongue) purchased from Riken Cell Bank (Tsukuba, Japan). The relative viable cell number was then determined by the MTT assay according to our previous studies [15,17,18,30,33,36−40]. The relative viable cell number was determined using a microplate reader (Sunrise Rainbow RC-R; TECAN, Männedorf, Switzerland). The concentration of compound that reduced the viable cell number by 50% (CC_{50}) was determined from the dose-response curve, and the mean value of CC_{50} for each cell type was calculated from triplicate assays as described before. Tumor-selectivity index (TS) was calculated using the following equation as TS = CC_{50} against HGF non-malignant cells/CC_{50} against malignant HSC-2 cells [(B/A)]. Potency-selectivity expression (PSE) was calculated using the following equation: PSE = [TS/(CC_{50} against tumor cells)] × 100 [that is, (B/A^2) × 100]. Experimental data are the mean ± standard deviation (SD). The statistical differences between control and treated groups were evaluated by paired Student's t-test. A value of $p < 0.05$ was considered to be significant.

4.4. Western blot assay

4.4.1. Reagents

RIPA buffer, a protease inhibitor cocktail was purchased from ATTO (Tokyo, Japan). Skim milk was purchased from Morinaga-Nyugyo (Tokyo, Japan). Quick Start Bradford protein assay kit was purchased from Bio-Rad Laboratories (Hercules, CA). Apoptosis Western Blot Cocktail kit was purchased from Abcam (Cambridge, UK). Amersham ECL Select was purchased from Cytiva (Tokyo, Japan).

4.4.2. Preparation of cell lysate

The incubation medium was removed to new microcentrifuge tubes from the cultured dish where cells are cultured. Then the tubes were spun at 10,000 g for 3 min. Precipitations were washed by ice-cold PBS twice and collected as floating cells. Adherent cells in the dishes, where the medium had been removed, were washed by ice-cold PBS twice. Next, the cells were incubated with RIPA buffer (1% NP-40, 0.5% sodium deoxycholate, 0.1% sodium dodecyl sulfate (SDS), 5 mM sodium deoxycholate, and 20 mM HEPES) containing protease inhibitor and phosphatase inhibitor cocktails in the dishes on the ice for 15 min. And then the cells were scraped with a scraper. The cell suspensions in RIPA buffer were transferred to the tubes where the floating cells have been collected. Both adherent and floating cells were incubated on the ice for 15 min. And then the tubes were centrifuged at 14,000×g for 10 min. Supernatants were collected as the cell lysate. Protein concentrations were determined with a Quick Start Bradford protein assay kit. The cell lysates were used for western blotting analysis.

4.4.3. Western blot analysis

All protein samples of cell lysates (10 μg) were separated by SDS-PAGE using a Mini-Protean 3 Cell system (Bio-Rad Laboratories). After electrophoresis, the separated proteins were transferred onto a PVDF filter using a Trans-Blot Turbo System (Bio-Rad Laboratories). The blots were blocked at room temperature for 50 min in skim milk and then probed for 120 min with a primary antibody cocktail (1:250) from Apoptosis Western Blot Cocktail kit. The blots were washed three times with Tris-buffered saline (pH 7.6) containing 0.05% Tween 20 and then probed for 90 min with horseradish peroxidase-conjugated secondary antibody cocktail (1:100) from the kit. Immunoreactivities were detected using Amersham ECL Select. Images were acquired using ChemiDoc MP System (Bio-Rad Laboratories) and Image Lab 4.1 software (Bio-Rad Laboratories). The exposure time was 0.275 or 10. 692 s.

4.5. QSAR analysis

We used the negative log CC_{50} (pCC_{50}) values for the comparison of cytotoxicity between compounds. The mean pCC_{50} values for

normal cells and tumor cell lines were defined as N and T, respectively. The difference (T−N) was used as a tumor-selectivity index [50]. Out of 2180 descriptors [354 Molecular Operating Environment (MOE) descriptors (version 2019.0101, Chemical Computing Group Inc., Quebec, Canada), 1826 Mordred descriptors [51]], descriptors with duplicate names, descriptors of the absolute value of 1 as internal correlation, missing descriptors, and descriptors that contain outliers based on Q1/4−3.0IQR ~ Q3/4 + 3.0IQR were removed. The remaining 1427 descriptors were used for the analysis. The CC_{50} values were expressed as mean ± S.D. of triplicate assays. Statistical analysis was done with JMP Pro15.0.0 (SAS Institute Inc. NC, USA). The significance level was set at $p < 0.05$.

4.6. Molecular docking

The *in silico* studies have been conducted using Schrödinger software [52]. Initially, all compounds including standard AZA were prepared using LigPrep tool [53] embedded in Schrödinger suite [52]. This tool generates all possible tautomer and ionization states using default conditions at pH 7.0 ± 2.0. Besides, several possible stereoisomers for each ligand while preserving the specified chiralities were also formed. The default force field used in all calculations was optimized potential liquid simulations 3e (OPLS3e) [54].

Our previously generated models [18] were used for docking of the ligands in the binding site of target enzymes which were high-resolution protein crystal structures of hCA I (2NMX; 1.55 Å), hCA II (3HS4; 1.10 Å), and hCA IX (3IAI; 2.20 Å). Glide extra precision (Glide XP) [55] was used for molecular docking.

Declaration of competing interest

The authors declare that they have no known competing financial interests or personal relationships that could have appeared to influence the work reported in this paper.

Acknowledgments

Dr. Cem Yamali was supported by the Scientific and Technological Research Council of Turkey, Turkey (TUBITAK) under 2214-A International Ph.D. Research Scholarship Program (1059B141601251-2214-A) and Ataturk University BAP office, Turkey (PRJ2017/10). Authors gratefully thank Serkan Levent (Anadolu University, Turkey) for HRMS analysis and Ataturk University, Department of Chemistry, Turkey for NMR analysis.

Appendix A. Supplementary data

Supplementary data to this article can be found online at https://doi.org/10.1016/j.ejmech.2021.113351.

References

[1] WHO Report on Cancer: Setting Priorities, Investing Wisely and Providing Care for All, World Health Organization, Geneva, 2020, pp. 1−160.
[2] Q.Y. Meng, H.L. Cong, H. Hu, F.J. Xu, Rational design and latest advances of codelivery systems for cancer therapy, Mater Today Bio 7 (2020) 100056.
[3] V. Alterio, A. Di Fiore, K. D'Ambrosio, C.T. Supuran, G. De Simone, Multiple binding modes of inhibitors to carbonic anhydrases: how to design specific drugs targeting 15 different isoforms? Chem. Rev. 112 (2012) 4421−4468.
[4] S. Pastorekova, S. Parkkila, J. Pastorek, C.T. Supuran, Carbonic anhydrases: current state of the art, therapeutic applications and future prospects, J. Enzyme Inhib. Med. Chem. 19 (2004) 199−229.
[5] R.G. Gieling, K.J. Williams, Carbonic anhydrase IX as a target for metastatic disease, Bioorg. Med. Chem. 21 (2013) 1470−1476.
[6] O. Ozensoy Guler, C.T. Supuran, C. Capasso, Carbonic anhydrase IX as a novel candidate in liquid biopsy, J. Enzyme Inhib. Med. Chem. 35 (2020) 255−260.
[7] A.M. Alafeefy, H.A. Abdel-Aziz, D. Vullo, A.M. Al-Tamimi, A.S. Awaad, M.A. Mohamed, C. Capasso, C.T. Supuran, Inhibition of human carbonic anhydrase isozymes I, II, IX and XII with a new series of sulfonamides incorporating aroylhydrazone-, [1,2,4]triazolo[3,4-b][1,3,4]thiadiazinyl- or 2-(cyanophenylmethylene)-1,3,4-thiadiazol-3(2H)-yl moieties, J. Enzyme Inhib. Med. Chem. 30 (2015) 52−56.
[8] M.A. Said, W.M. Eldehna, A. Nocentini, S.H. Fahim, A. Bonardi, A.A. Elgazar, V. Krystof, D.H. Soliman, H.A. Abdel-Aziz, P. Gratteri, S.M. Abou-Seri, C.T. Supuran, Sulfonamide-based ring-fused analogues for CAN508 as novel carbonic anhydrase inhibitors endowed with antitumor activity: design, synthesis, and in vitro biological evaluation, Eur. J. Med. Chem. 189 (2020) 112019.
[9] K.K. Sethi, S.M. Verma, A systematic quantitative approach to rational drug design and discovery of novel human carbonic anhydrase IX inhibitors, J. Enzyme Inhib. Med. Chem. 29 (2014) 571−581.
[10] A.I. Lorenzo-Pouso, M. Gallas-Torreira, M. Perez-Sayans, C.M. Chamorro-Petronacci, O. Alvarez-Calderon, B. Takkouche, C.T. Supuran, A. Garcia-Garcia, Prognostic value of CAIX expression in oral squamous cell carcinoma: a systematic review and meta-analysis, J. Enzyme Inhib. Med. Chem. 35 (2020) 1258−1266.
[11] J.S. Yang, C.W. Lin, Y.H. Hsieh, M.H. Chien, C.Y. Chuang, S.F. Yang, Overexpression of carbonic anhydrase IX induces cell motility by activating matrix metalloproteinase-9 in human oral squamous cell carcinoma cells, Oncotarget 8 (2017) 83088−83099.
[12] A.W. Eckert, S. Horter, D. Bethmann, J. Kotrba, T. Kaune, S. Rot, M. Bache, U. Bilkenroth, W. Reich, T. Greither, C. Wickenhauser, D. Vordermark, H. Taubert, M. Kappler, Investigation of the prognostic role of carbonic anhydrase 9 (CAIX) of the cellular mRNA/Protein level or soluble CAIX protein in patients with oral squamous cell carcinoma, Int. J. Mol. Sci. 20 (2019) 375.
[13] N.T. Brockton, A.C. Klimowicz, P. Bose, S.K. Petrillo, M. Konno, L. Rudmik, M. Dean, S.C. Nakoneshny, T.W. Matthews, S. Chandarana, H.Y. Lau, A.M. Magliocco, J.C. Dort, High stromal carbonic anhydrase IX expression is associated with nodal metastasis and decreased survival in patients with surgically-treated oral cavity squamous cell carcinoma, Oral Oncol. 48 (2012) 615−622.
[14] C.W. Lin, W.E. Yang, W.J. Lee, K.T. Hua, F.K. Hsieh, M. Hsiao, C.C. Chen, J.M. Chow, M.K. Chen, S.F. Yang, M.H. Chien, Lipocalin 2 prevents oral cancer metastasis through carbonic anhydrase IX inhibition and is associated with favourable prognosis, Carcinogenesis 37 (2016) 712−722.
[15] H.I. Gul, E. Mete, S.E. Eren, H. Sakagami, C. Yamali, C.T. Supuran, Designing, synthesis and bioactivities of 4-[3-(4-hydroxyphenyl)-5-aryl-4,5-dihydropyrazol-1-yl]benzenesulfonamides, J. Enzyme Inhib. Med. Chem. 32 (2017) 169−175.
[16] H.I. Gul, C. Yamali, M. Bulbuller, P.B. Kirmizibayrak, M. Gul, A. Angeli, S. Bua, C.T. Supuran, Anticancer effects of new dibenzenesulfonamides by inducing apoptosis and autophagy pathways and their carbonic anhydrase inhibitory effects on hCA I, hCA II, hCA IX, hCA XII isoenzymes, Bioorg. Chem. 78 (2018) 290−297.
[17] H.I. Gul, C. Yamali, H. Sakagami, A. Angeli, J. Leitans, A. Kazaks, K. Tars, D.O. Ozgun, C.T. Supuran, New anticancer drug candidates sulfonamides as selective hCA IX or hCA XII inhibitors, Bioorg. Chem. 77 (2018) 411−419.
[18] C. Yamali, H.I. Gul, A. Ece, S. Bua, A. Angeli, H. Sakagami, E. Sahin, C.T. Supuran, Synthesis, biological evaluation and in silico modelling studies of 1,3,5-trisubstituted pyrazoles carrying benzenesulfonamide as potential anticancer agents and selective cancer-associated hCA IX isoenzyme inhibitors, Bioorg. Chem. 92 (2019) 103222.
[19] A.A. Abdel-Aziz, A.S. El-Azab, M.A. Abu El-Enin, A.A. Almehizia, C.T. Supuran, A. Nocentini, Synthesis of novel isoindoline-1,3-dione-based oximes and benzenesulfonamide hydrazones as selective inhibitors of the tumor-associated carbonic anhydrase IX, Bioorg. Chem. 80 (2018) 706−713.
[20] H.A. Allam, S.H. Fahim, F.A.-A. M, A. Nocentini, M.E. Elbakry, M.A. Abdelrahman, W.M. Eldehna, H.S. Ibrahim, C.T. Supuran, Application of hydrazino and hydrazido linkers to connect benzenesulfonamides with hydrophilic/phobic tails for targeting the middle region of human carbonic anhydrases active site: selective inhibitors of hCA IX, Eur. J. Med. Chem. 179 (2019) 547−556.
[21] S. Singh, C.L. Lomelino, M.Y. Mboge, S.C. Frost, R. McKenna, Cancer drug development of carbonic anhydrase inhibitors beyond the active site, Molecules 23 (2018).
[22] V. Alterio, A. Di Fiore, K. D'Ambrosio, C.T. Supuran, G. De Simone, Multiple binding modes of inhibitors to carbonic anhydrases: how to design specific drugs targeting 15 different isoforms? Chem. Rev. 112 (2012) 4421−4468.
[23] A study of SLC-0111 and gemcitabine for metastatic pancreatic ductal cancer in subjects positive for CAIX (SLC-0111-17-01). https://clinicaltrials.gov/ct2/show/NCT03450018, 2020.
[24] F. Carta, D. Vullo, S.M. Osman, Z. AlOthman, C.T. Supuran, Synthesis and carbonic anhydrase inhibition of a series of SLC-0111 analogs, Bioorg. Med. Chem. 25 (2017) 2569−2576.
[25] D. Moi, A. Nocentini, A. Deplano, S.M. Osman, Z.A. AlOthman, V. Piras, G. Balboni, C.T. Supuran, V. Onnis, Appliance of the piperidinyl-hydrazidoureido linker to benzenesulfonamide compounds: synthesis, in vitro and in silico evaluation of potent carbonic anhydrase II, IX and XII inhibitors, Bioorg. Chem. 98 (2020) 103728.
[26] V. Sharma, R. Kumar, S. Bua, C.T. Supuran, P.K. Sharma, Synthesis of novel benzenesulfonamide bearing 1,2,3-triazole linked hydroxy-trifluoromethylpyrazolines and hydrazones as selective carbonic anhydrase isoforms IX and XII inhibitors, Bioorg. Chem. 85 (2019) 198−208.

[27] Kübra Demir-Yazıcı, Silvia Bua, Nurgül Mutlu Akgüneş, Atilla Akdemir, Claudiu T. Supuran, Özlen Güzel-Akdemir, Indole-based hydrazones containing A sulfonamide moiety as selective inhibitors of tumor-associated human carbonic anhydrase isoforms IX and XII, Int. J. Mol. Sci. 20 (2019) 2354.
[28] S. Iqbal, M. Saleem, M.K. Azim, M. Taha, U. Salar, K.M. Khan, S. Perveen, M.I. Choudhary, Carbohydrazones as new class of carbonic anhydrase inhibitors: synthesis, kinetics, and ligand docking studies, Bioorg. Chem. 72 (2017) 89–101.
[29] K. Kucukoglu, H.I. Gul, P. Taslimi, I. Gulcin, C.T. Supuran, Investigation of inhibitory properties of some hydrazone compounds on hCA I, hCA II and AChE enzymes, Bioorg. Chem. 86 (2019) 316–321.
[30] H.I. Gul, C. Yamali, Synthesis of potential anticancer effective compounds containing pyrazole-benzensulfonamide moieties, enlightenment of their structures and their cytotoxic activities, PCT Int. Appl. (2019) 1–36. WO 2019017857 A2 20190124.
[31] H.I. Gul, C. Yamali, A. Tugce Yasa, E. Unluer, H. Sakagami, M. Tanc, C.T. Supuran, Carbonic anhydrase inhibition and cytotoxicity studies of Mannich base derivatives of thymol, J. Enzyme Inhib. Med. Chem. 31 (2016) 1375–1380.
[32] R.G. Khalifah, The carbon dioxide hydration activity of carbonic anhydrase. I. Stop-flow kinetic studies on the native human isoenzymes B and C, J. Biol. Chem. 246 (1971) 2561–2573.
[33] C. Yamali, H.I. Gul, H. Sakagami, C.T. Supuran, Synthesis and bioactivities of halogen bearing phenolic chalcones and their corresponding bis Mannich bases, J. Enzyme Inhib. Med. Chem. 31 (2016) 125–131.
[34] C. Yamali, M. Tugrak, H.I. Gul, M. Tanc, C.T. Supuran, The inhibitory effects of phenolic Mannich bases on carbonic anhydrase I and II isoenzymes, J. Enzyme Inhib. Med. Chem. 31 (2016) 1678–1681.
[35] J.Y. Winum, A. Maresca, F. Carta, A. Scozzafava, C.T. Supuran, Polypharmacology of sulfonamides: pazopanib, a multitargeted receptor tyrosine kinase inhibitor in clinical use, potently inhibits several mammalian carbonic anhydrases, Chem Commun (Camb). 48 (2012) 8177–8179.
[36] S. Bilginer, H.I. Gul, F.S. Erdal, H. Sakagami, S. Levent, I. Gulcin, C.T. Supuran, Synthesis, cytotoxicities, and carbonic anhydrase inhibition potential of 6-(3-aryl-2-propenoyl)-2(3H)-benzoxazolones, J. Enzyme Inhib. Med. Chem. 34 (2019) 1722–1729.
[37] H.I. Gul, M. Tugrak, M. Gul, H. Sakagami, N. Umemura, B. Anil, Synthesis and cytotoxicities of new azafluorenones with apoptotic mechanism of action and cell cycle analysis, Anticancer Agents Med. Chem. 18 (2018) 1770–1778.
[38] H.I. Gul, M. Tugrak, H. Sakagami, P. Taslimi, I. Gulcin, C.T. Supuran, Synthesis and bioactivity studies on new 4-(3-(4-Substitutedphenyl)-3a,4-dihydro-3H-indeno[1,2-c]pyrazol-2-yl) benzenesulfonamides, J. Enzyme Inhib. Med. Chem. 31 (2016) 1619–1624.
[39] M. Tugrak, C. Yamali, H. Sakagami, H.I. Gul, Synthesis of mono Mannich bases of 2-(4-hydroxybenzylidene)-2,3-dihydroinden-1-one and evaluation of their cytotoxicities, J. Enzyme Inhib. Med. Chem. 31 (2016) 818–823.
[40] C. Yamali, H.I. Gul, D.O. Ozgun, H. Sakagam, N. Umemura, C. Kazaz, M. Gul, Synthesis and cytotoxic activities of difluoro-dimethoxy chalcones, Anticancer Agents Med. Chem. 17 (2017) 1426–1433.
[41] L. Llorach-Pares, A. Nonell-Canals, M. Sanchez-Martinez, C. Avila, Computer-aided drug design applied to marine drug discovery: meridianins as alzheimer's disease therapeutic agents, Mar. Drugs 15 (2017).
[42] P. Sledz, A. Caflisch, Protein structure-based drug design: from docking to molecular dynamics, Curr. Opin. Struct. Biol. 48 (2018) 93–102.
[43] A. Ece, Towards more effective acetylcholinesterase inhibitors: a comprehensive modelling study based on human acetylcholinesterase protein-drug complex, J. Biomol. Struct. Dyn. 38 (2020) 565–572.
[44] K. Chan, N. Frankish, T. Zhang, A. Ece, A. Cannon, J. O'Sullivan, H. Sheridan, Bioactive indanes: insight into the bioactivity of indane dimers related to the lead anti-inflammatory molecule PH46A, J. Pharm. Pharmacol. 72 (2020) 927–937.
[45] A. Ece, B. Pejin, A computational insight into acetylcholinesterase inhibitory activity of a new lichen depsidone, J. Enzyme Inhib. Med. Chem. 30 (2015) 528–532.
[46] A. Ece, F. Sevin, Exploring QSAR on 4-cyclohexylmethoxypyrimidines as antitumor agents for their inhibitory activity of cdk2, Lett. Drug Des. Discov. 7 (2020) 625–631.
[47] A. Maryam, R.R. Khalid, S.C. Vedithi, A. Ece, S.S. Cinaroglu, A.R. Siddiqi, T.L. Blundell, Exploring the structural basis of conformational heterogeneity and autoinhibition of human cGMP-specific protein kinase Ialpha through computational modelling and molecular dynamics simulations, Comput. Struct. Biotechnol. J. 18 (2020) 1625–1638.
[48] M. Er, A.M. Abounakhla, H. Tahtaci, A.H. Bawah, S.S. Cinaroglu, A. Onaran, A. Ece, An integrated approach towards the development of novel antifungal agents containing thiadiazole: synthesis and a combined similarity search, homology modelling, molecular dynamics and molecular docking study, Chem. Cent. J. 12 (2018) 121.
[49] H.I. Gul, C. Yamali, Synthesis of pyrazol-benzensulfonamide containing anticancer effective compound having cytotoxic activity, Turk. Pat. Appl. (2017) 1–34. TR 2017006371 A2 20170921.
[50] Y. Uesawa, H. Sakagami, M. Ishihara, H. Kagaya, T. Kanamoto, S. Terakubo, H. Nakashima, H. Yahagi, K. Takao, Y. Sugita, Quantitative structure-cytotoxicity relationship of 3-styryl-2H-chromenes, Anticancer Res. 35 (2015) 5299–5307.
[51] H. Moriwaki, Y.S. Tian, N. Kawashita, T. Takagi, Mordred: a molecular descriptor calculator, J. Cheminf. 10 (2018) 4.
[52] Schrödinger, Small-Molecule Drug Discovery Suite, Schrödinger, LLC, New York, NY, 2020.
[53] Schrödinger, LigPrep, Schrödinger, LLC, New York, NY, 2020.
[54] E. Harder, W. Damm, J. Maple, C. Wu, M. Reboul, J.Y. Xiang, L. Wang, D. Lupyan, M.K. Dahlgren, J.L. Knight, J.W. Kaus, D.S. Cerutti, G. Krilov, W.L. Jorgensen, R. Abel, R.A. Friesner, OPLS3: a force field providing broad coverage of drug-like small molecules and proteins, J. Chem. Theor. Comput. 12 (2016) 281–296.
[55] R.A. Friesner, R.B. Murphy, M.P. Repasky, L.L. Frye, J.R. Greenwood, T.A. Halgren, P.C. Sanschagrin, D.T. Mainz, Extra precision glide: docking and scoring incorporating a model of hydrophobic enclosure for protein-ligand complexes, J. Med. Chem. 49 (2006) 6177–6196.